OMEGA EP
System Operations Manual
Volume VII–System Description
Chapter 5: Optomechanical System

Chapter 5
Optomechanical System

5.0 INTRODUCTION

The Optomechanical System is defined as the optics and optomechanical support hardware necessary to transport the laser beams through the system from the Laser Sources output pulse to the target. The optical system meets the system performance requirements described in Chap. 1: System Overview, S-AD-M-005, and consists of the following subsystems: seed-pulse injection from laser sources into the amplifier, the laser amplifier cavity and fold mirrors, spatial filters, beam switchyard, and the short- and long-pulse beam paths that involve either pulse compression or frequency conversion, respectively, and final transport into the target chamber.

The Optomechanical System starts at the final apodizer image plane produced by the Laser Sources Subsystem and ends with the final focusing optics within either the OMEGA or the OMEGA EP target chamber (Fig. 5.1). Figure 5.2 shows a schematic of the main portions of the Optomechanical System.

The laser system is designed to operate in either short-pulse or long-pulse configuration. Short-pulse configuration is possible with Beamlines 1 and 2, while all four beamlines support long-pulse operation. Short-pulses (1 to 100 ps) originate in the Laser Sources Subsystem as frequency-chirped pulses that are then amplified and directed into a pulse compressor where they are temporally compressed before being imaged onto the target. Short pulses are then delivered to either the OMEGA or OMEGA EP target chambers with up to 2.6 kJ of energy.

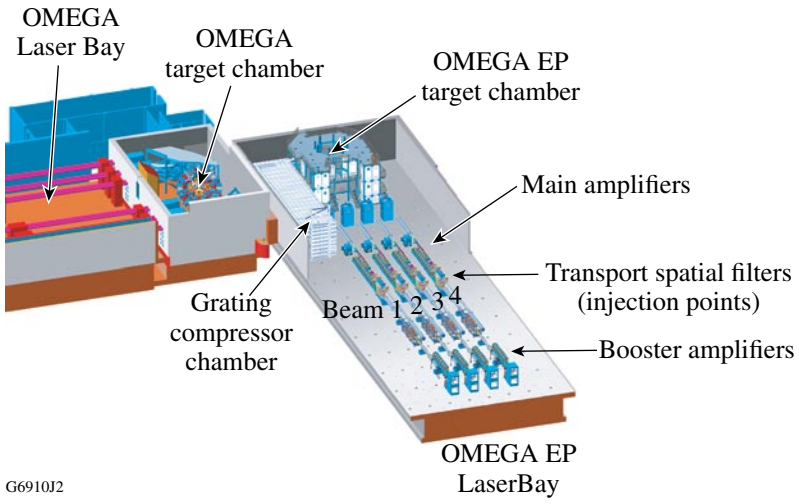

Figure 5.1
OMEGA EP Optomechanical System starts in Laser Sources with injection of the pulse and ends in either the OMEGA or OMEGA EP Target Chamber. OMEGA EP has four beamlines.

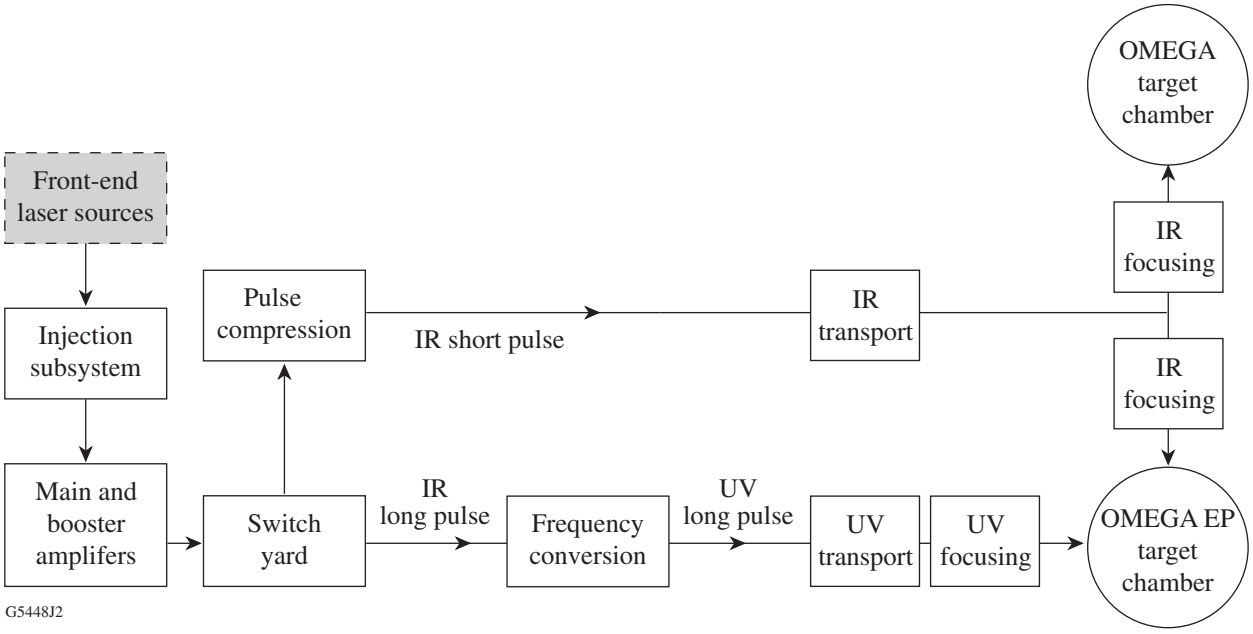

Figure 5.2
Schematic of the main portions of the OMEGA EP Optomechanical System.

Long pulses (1 to 10 ns) originate in the laser sources of all four beamlines and are subsequently amplified and frequency converted from 1ω to 3ω (351 nm) before being imaged onto the target. Long pulses are directed to the OMEGA EP target chamber. Each beamline operates independently.

The structural system includes the mechanical support systems and mounts for the optical components and systems. The major structures serve as the stable support interface between all of the optical hardware and the Laser Bay floor.

The beamlines are folded with the transport spatial filter (TSF) and booster amplifier residing above the main amplifier and cavity spatial filter. This design results in a shorter focal-length TSF lens than that used on the National Ignition Facility (NIF).

The need for short pulses introduces optical requirements that include a grating-based pulse compressor and reflective focusing optics. Appendix A lists the Optomechanical System's optical components and their primary specifications. The definitions of clear aperture and related terms are given in Fig. 5.3. The requirements of the optical components are outlined in Sec. 5.1, and their detailed applications are described in Sec. 5.2. The structural and vacuum systems are described in Sec. 5.3.

The Laser Sources Subsystem is described in Chap. 2: Laser Sources, S-AD-M-006. Details of the laser amplifiers are described in Chap. 3: Laser Amplifiers, S-AD-M-007. Infrared, ultraviolet, and short-pulse diagnostic instruments are described in Chap. 6: Laser Diagnostics, S-AD-M-010.

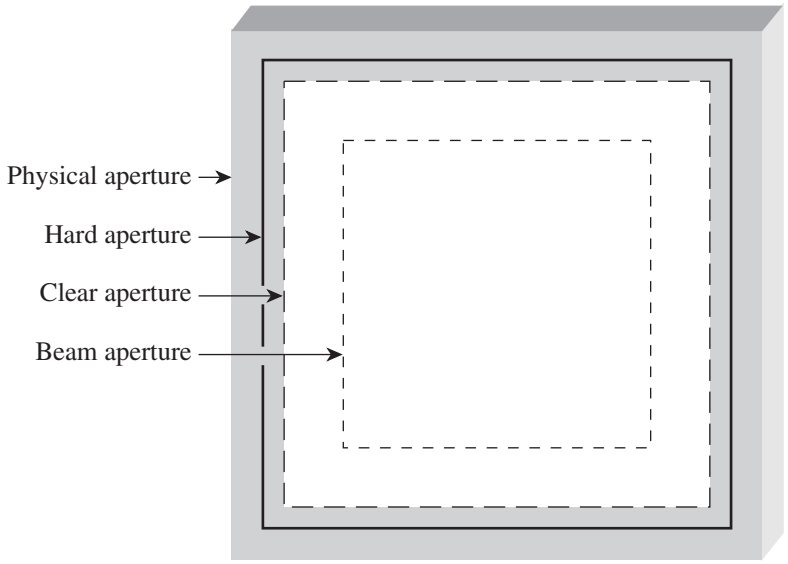

Figure 5.3
Aperture definitions.

Physical aperture: actual outer dimensions of the optical component
Hard aperture: limiting aperture defined by the mechanical mount interface
Clear aperture: area of component over which all optical specifications apply
Beam aperture: dimension at which the beam intensity is 1% of the peak intensity

G5533J1

5.1 BEAMLINE REQUIREMENTS

The Optomechanical System has been designed to satisfy the following functional requirements:

- The input beam from the Laser Sources subsystem is magnified to a ~37-cm-sq aperture within the laser cavity and this dimension is maintained throughout transport to the focusing optics at the target chamber.

- Beams following each amplification stage are spatially filtered to remove diffraction modulation that contribute to near-field nonuniformities and self-focusing.

- The image of the apodizer located in the Laser Sources subsystem used to create the square beam profile is relayed by 1:1 spatial filters to key locations to minimize diffraction modulation and maintain an optimal spatial profile.

- Long-pulse infrared (IR) and ultraviolet (UV) beams and short-pulse IR beams are transported with sufficient fluences to meet the top-level specifications for on-target energy (5 kJ/beam for long-pulse UV beams and up to 2.6 kJ for short-pulse IR beams).

- The two coaxial short-pulse beams can be routed to either the OMEGA or the OMEGA EP target chamber and can also be configured to independently illuminate the target in the OMEGA EP target chamber as a backlighter and a sidelighter beam.

- Long-pulse IR beams are frequency tripled from 1053 nm (IR) to 351 nm (UV).

- The four long-pulse beams can be routed to the OMEGA EP target chamber.

- Pulse compression is provided for the two short-pulse beamlines. Either can be compressed to pulse widths as short as 1 ps. However, the pulse in the lower compressor is limited in pulse width or energy when it passes through the beam combiner, due to the *B*-integral limitations of the optic.

- Pre-shot adaptive-optic correction of thermally induced wavefront errors caused by the amplifier disks and static wavefront errors introduced by optical components including the compression gratings is provided by deformable mirrors located in the amplifier cavity and the pulse compressor.

To service the system and provide the means to verify that the above requirements are being met, the diagnostic system has the capabilities to

- accurately and precisely align beams to 6.8 μrad (short pulse) and 9.3 μrad (long pulse) at 1 σ in pointing;
- measure the on-target IR energy of each short-pulse beam;
- measure the on-target UV energy of each long-pulse beam;
- measure the total output energy of the first, second, and third harmonic of each long-pulse beam;
- measure the pulse shape and pulse contrast;
- measure the near-field wavefront quality at key image planes in the beam path;
- measure the wavefront quality at key image planes in the beam path; and
- measure the far-field spot profile at and near the focal plane of the focusing optics.

5.2 OPTICAL SYSTEM DESIGN

5.2.1 System Design Basis

The system configuration is based upon a design that meets the system requirements as specified in the OMEGA EP System and Configuration Requirements document, S-AA-G-05, and the Optical Design Configuration, Beamlines, S-AC-G-015. System level budgets were developed for energy, S-AC-X-006, wavefront, S-AC-X-004, and alignment, S-AC-X-017 (centering) and S-AC-X-005 (pointing). Each budget was then distributed among discrete subsystems to formulate requirements for their independent design. Each subsystem was then broken down into its components and the budgets were allocated for each assembly. Then each was apportioned to provide tolerances for each major step in the component production process (substrate finishing, coating, mounting, and alignment). Tolerance allocations were also made for holographic errors associated with the production of diffraction gratings and prompt-induced distortion (PID) of the amplifier disks.

The allowable wavefront error for each component at each stage of manufacture was specified from these allocations so that the system is capable of focusing 80% of the encircled energy within a 10-μm radius at the final focus of the beam. Table 5.1 shows a breakdown of the budget by subsystem for Beamline 1 or 2 when configured in short-pulse mode.

Table 5.2 shows a breakdown of the budget by subsystem for Beamline 3 or 4 when configured in long-pulse mode (Beamlines 1 and 2 in long-pulse mode are similar). Note that compared to the short-pulse requirements, the required focal-spot size was allowed to increase to a 50-μm radius.

Table 5.1: Wavefront budget subsystem allocation(a) for Beamline 1 or 2 in short-pulse configuration.

Subsystem	Budget allocation (μrad)	Spot radius (μm)	DM[(b)]	Mag[(c)]	Local (μrad)	Spot radius (μm)
Design error	2.56	2.67	1.0	1.0	2.56	2.67
Chromatic error	4.50	4.70	1.0	1.0	4.50	4.70
Laser sources	3.50	3.65	1.0	6.3	22.0	
Injection	1.02	1.06	1.0	6.3	6.42	
Beamline optics	3.91	4.08	6.4	1.0	25.1	26.20
PID[(d)]	3.59	3.75	10.0	1.0	35.9	37.46
Gratings (G1–G4)	1.48	1.55	4.0	1.0	5.93	6.19
Beam combiner through OAP	1.52	1.58	7.0	1.0	10.61	11.07
B-integral sum	3.56	3.71	1.0	1.0	3.56	3.71
Margin[(e)]	2.53	2.64	1.0	1.0	2.53	2.64
RSS[(f)] divergence	9.58	10.00			51.36	47.96

[(a)]Allocation is based on top-level requirements of 80% encircled energy, 10-μm radius, OAP focal length of 1.044 m, and divergence of 9.58 μrad.
[(b)]Deformable mirror correction factor
[(c)]Local beam magnification
[(d)]Prompt-induced distortion from amplifier disks
[(e)]Diffraction limit = 1 spot
[(f)]Root-sum-squared

Table 5.2: Wavefront budget subsystem allocation[(a)] for Beamline 3 or 4 in long-pulse configuration.

Subsystem	Budget allocation (μrad)	Spot radius (μm)	DM(b)	Mag(c)	Local (μrad)	Spot radius (μm)
Design error	0.97	3.29	1.0	1.0	0.97	3.29
Chromatic error	1.00	3.39	1.0	1.0	1.00	3.39
Laser sources	3.50	11.88	1.0	6.3	22.0	
Injection	1.02	3.46	1.0	6.3	6.42	
Main laser	3.91	13.26	6.4	1.0	25.1	85.02
PID[(d)]	3.59	12.18	10.0	1.0	35.9	121.83
Transport	2.45	8.30	1.0	1.0	2.45	8.30
FCC's through focusing	6.72	22.82	1.0	1.0	6.72	22.82
B-integral sum	8.79	29.83	1.0	1.0	8.79	29.83
Margin[(e)]	6.72	22.82	1.0	1.0	6.72	22.82
RSS[(f)] divergence	14.73	50.00			51.18	155.22

[(a)]Allocation is based on top-level requirements of 80% encircled energy, 50-μm radius, focal length of 3.4 m, and divergence of 14.73 μrad.
[(b)]Deformable mirror correction factor
[(c)]Local beam magnification
[(d)]Prompt-induced distortion from amplifier disks
[(e)]Diffraction limit = 1 spot
[(f)]Root-sum-squared

The energy budget specifies the beam fluence at various points in the system, thereby impacting the choice of substrate material, typically BK-7 or fused silica, and their high-reflection (HR) or antireflection (AR) coating requirements.

Four key constraints drove the design of the optomechanical assemblies. (1) Strain-free mounting of all optical components within a subframe. The subframe is a simply supported, outer-edge-perimeter–mounting scheme. The subframe-to-frame interface[1] generally consists of three-point, six degree-of freedom, exact-constraint designs that prevent optical distortion due to tolerance buildup from mount manufacturing, assembly, and environmental effects. (2) The need for precision pointing and centering control of optical components, including fixed mounts, manual drives, and motorized drives that typically have μm and/or μrad accuracy and stability requirements. (3) The need to provide an adjustment range adequate to center the laser beam within the clear aperture of each optic. The range must be sufficient to compensate for typical fabrication and structure installation tolerances. (4) All optical components must be packaged within the space allocated by the system configuration.

5.2.2 Optical System Description

An overview description of the optical system, starting at the Laser Sources was given in Fig. 5.2. The Laser Sources Subsystem is described in detail in the OMEGA EP Vol. VII, System Description, Chap. 2, Laser Sources, S-AD-M-006. The following sections provide an overview of the optical subsystems from the seed injection pulse through the main beamline, short- or long-pulse transport systems and into either the OMEGA or OMEGA EP target chambers.

- The Laser Sources are located in the Laser Sources Bay on the first floor of the facility. Each of the four beamlines is fed by an independent laser source, identified as LS1 to LS4. Beamlines 1 and 2 have the capability to operate in short-pulse or long-pulse mode and their sources have the ability to produce both types of pulses. Short pulses originate from a mode-locked oscillator that produces 220-fs pulses synchronized to the Reference Frequency Generator. Each pulse has a spectral bandwidth greater than 8 nm. These pulses are stretched in time using a grating-pulse stretcher and amplified using optical parametric chirped-pulse amplification (OPCPA). Long pulses originate in a narrowband, solid-state, fiber-based monomode oscillator and are amplified in a regenerative amplifier after temporal shaping. Either pulse is then injected into a larger-aperture glass amplifier that feeds the main amplification stages. Each type of pulse must satisfy a specific set of design requirements for its spatial-intensity distribution, temporal pulse shape, and spectral composition. Each source is equipped with a periscope that transports the pulse to the beamline injection table located in the Laser Bay.

- Each beamline is equipped with an injection table, an infrared alignment table (IRAT), and an infrared diagnostics package (IRDP) optical table. The sources pulse exits the top of the periscope onto the IRAT table where it is co-aligned with the IRAT laser. A portion of the beam is sampled to provide an energy measurement, and the main beam is aligned with a system cross-hair on the injection table. The alignment sensor package (ASP) on the injection table provides course and fine pointing and centering of the beam. A SI-800 Scientific camera provides near-field (NF) images, and an insertable calorimeter measures beam energy and provides a beam block to the optics chain leading to the injection mirror on the TSF pinhole region's optical table.

- The injection mirror directs the beam through the Pass-1 pinhole of the TSF to the input TSF lens where it has expanded to the 36.9-cm beam size that is maintained throughout the system (except when passing through TSF and CSF pinholes) until final focusing. The TSF lens collimates the pulse and directs it into the 7-disk booster amplifier (BA). The cavity fold mirror directs the beam down to the cavity polarizer (POL1) where the beam's polarization coupled with the coating design causes it to be reflected from the surface and through the plasma-electrode Pockels cell (PEPC) that is switched OFF. Located between the PEPC and the cavity spatial filter (CSF) in Beamlines 1 and 2 are the short-pulse polarizers [POL2[(a)]], where the beam is polarized so that it transmits through the polarizer and on to the CSF's Pass-1 pinhole and the 11-disk main amplifier, to reach the end of the beamline at the deformable mirror (DM). The DM has been calibrated and the mirror surface deformed to account for the PID of the amplifiers. Nitrogen-filled beam tubes between the elements maintain an inert, dry atmosphere, preventing the amplifier reflectors from oxidation and maintaining the correct environment for the thin-film coatings of the polarizers and mirrors.

- There are two options for the beam on the return pass. One option traps the beam in the cavity by switching ON the PEPC, rotating the beam polarization 90°, and allowing the beam to transmit through POL1 where it reflects off the cavity end mirror (CEM). The CEM reflects the beam back through POL1, the PEPC (still switched ON), and the CSF Pass-3 pinhole to the DM. By this time, the PEPC has switched OFF, and on the fourth pass through the cavity, the beam exits by reflecting off POL1. The beam then reflects off the cavity fold mirror through the BA, the TSF's Pass-4 pinhole, and into the switchyard. The second option uses the DM to point the beam to the Pass-2 pinhole in the CSF and similarly and subsequently exiting the TSF and entering the switchyard.

- Exiting the TSF, the beam passes through the IR diagnostic beamsplitter (IR-DBS) where a small portion (~0.2%) is reflected back into the TSF where it is collimated before being directed to the IRDP for characterization.

- After exiting the TSF, the beam enters a switchyard. Beams 1 and 2 may be directed into the grating compressor chamber (GCC) if they are short-pulse beams, or to the frequency-conversion crystals (FCC's) if they are long-pulse beams. Additionally, Beams 1 and 2 may be directed to either pulse compressor located within the GCC. Insertable full-aperture calorimeters are also mounted on the structures and removed for target shots. The following two sections describe the respective short- and long-pulse beam paths.

5.2.2.1 Short-pulse beam transport

The short-pulse beam transport includes the GCC, transport from the GCC to the target chamber, and focusing on target.

- Short-pulse beams are directed into the GCC where they enter either the upper- or lower-pulse compressor (depending upon the switchyard configuration) from the east side. The GCC is a large stainless steel vacuum vessel located in the northwest corner of the Target Bay, measuring 70-ft long and 15-ft square and operated at a vacuum of ~1×10^{-6} Torr. Within

[(a)]POL2 is used on the two short-pulse beamlines to divert retroreflections from the target into an attached dump. The beam dump may be interchanged with a full-aperture calorimeter for energy measurements.

the GCC, optical tables are arranged in four cells. Cell 4 is the most southern and consists of four optical tables, two each for the upper and lower pulse compressor. Cell 3 is a similar design, residing to the north of Cell 4. Cell 2 has a single upper and lower table and, at the north end, Cell 1 consists of four tables. Cell 1 supports a complex suite of optics (see Fig. 5.4)

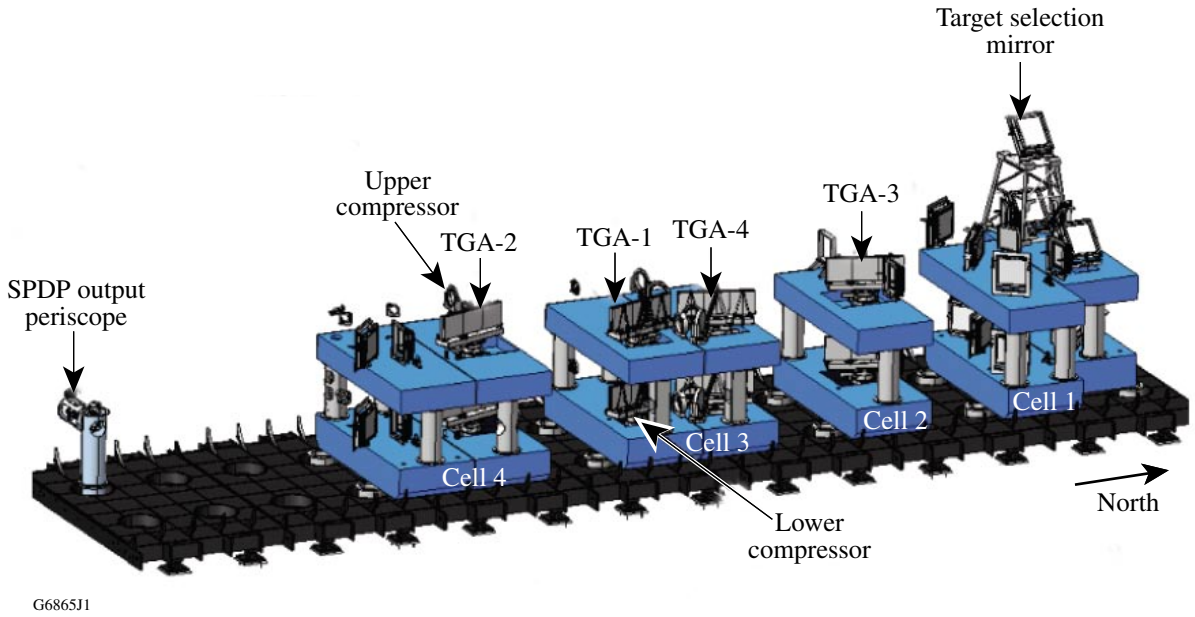

Figure 5.4
The inner workings of the GCC show the locations of the TGA's—TGA1 to TGA4—and the target chamber selection mirror. The upper and lower compressors for Beams 1 and 2 are positioned atop one another. After pulse compression, the co-aligned beams reflect off the selection mirror and exit the GCC, propagating to the target chamber of choice. Diagnostic beams exit the GCC via the short-pulse diagnostic package (SPDP) output periscope.

that reflect the compressed pulses from each beamline to a target chamber selection mirror and also supports two DM's and two full-aperture calorimeters.

- A pulse compressor temporally compresses each of the beams. The pulse compressor is a dispersive delay device where the path lengths of longer wavelengths of light are greater than those of shorter wavelengths. Pulse-compression techniques achieve short-pulse energy-on-target (EOT) levels of 2.6 kJ with a pulse width of 1 to 100 ps into a 10-μm focal-spot radius on target.

- Each pulse compressor consists of four tiled-grating assemblies (TGA's) arranged in a "bow-tie" pattern (see Fig. 5.5). The upper compressor is located above the lower compressor on a separate optical table. Each TGA is comprised of a 1×3 array of multilayer dielectric (MLD) grating tiles having a line spacing of 1740 l/mm (see Fig. 5.6). Maintaining focusability puts stringent alignment requirements on the outboard tiles relative to a fixed center tile. While the separation of the compressor gratings remains fixed, the output pulse widths of the two compressed beams can be adjusted over a range of 1 to 100 ps by adjusting the pulse stretcher in Laser Sources. These pulse-width changes can be made within a shot cycle (2 h). The TGA's are numbered sequentially relative to their propagation throughout the compressor (TGA1 to TGA4).

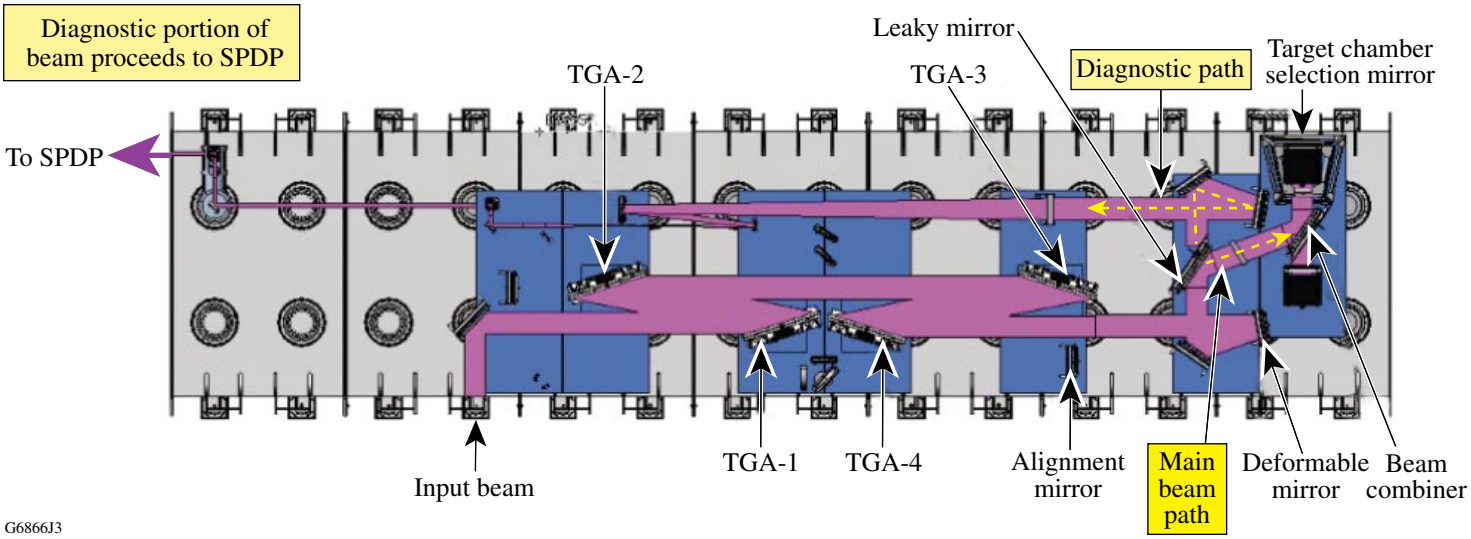

Figure 5.5
The upper compressor's optical path includes the deformable mirror, beam combiner, and target chamber selection mirror. The diagnostic mirror provides a 1% pickoff for the SPDP, shown exiting the chamber to the left. The optical configuration of the lower compressor is similar. The circles in the drawing are the GCC floor attachments.

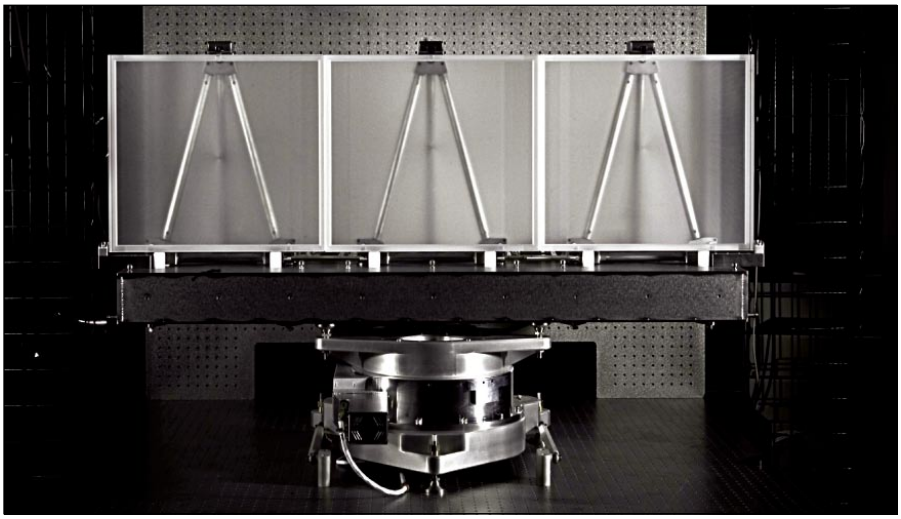

Figure 5.6
The photograph shows the three tiled gratings aligned on the optical support beam and supported by a rotary stage used for coarse alignment. Each of the outboard tiles has a precision control system used to align the beam wavefront to that of the center grating tile.

- TGA1 is oriented at 72.5° relative to the incoming beam. This pulse (~1 ns) has ~3.5 nm of bandwidth that is angularly dispersed into its spectral components and propagated to TGA2 located 3.08 m away. From TGA2, the beam is then propagated 8.3 m to TGA3. Diffracting from TGA3, the spectral components are recombined after diffracting from TGA4, 3.38 m away. (The slight offset in spacing between grating pairs reduces near-field modulation by leaving a small amount of residual spatial chirp.) The longer wavelengths travel a greater

path length through the compressor than the shorter wavelengths by the time they have reached TGA4, compressing in time the width of the pulse.

- Emerging from the compressor, the pulse reflects off a DM to compensate for aberrations in the system. The pulse then reflects off a fold mirror and then off the surface of a diagnostic beamsplitter where a sample of the beam is diverted to an optical chain leading out of the GCC to the short-pulse diagnostics table. A full-aperture calorimeter may be inserted into the optical path after the leaky mirror to measure the energy in the beam.

- A configuration option enables the upper compressor pulse to be directed to the OMEGA EP backlighter port of the target chamber (TC) and the lower compressor pulse to be directed to the sidelighter port. Alternatively, the beams are directed to a beam-combiner optic where the lower compressor pulse is transmitted and the upper compressor pulse is reflected, causing the beams to become co-axial (although temporally separated). A target chamber selection mirror directs the combined beams through an evacuated beam tube to the selected chamber via a pair of transport mirrors. Either the OMEGA or OMEGA EP backlighter path may be selected.

- A pair of mirrors (SPHR5 and 6) transports the beam through the shield wall and into the OMEGA TC. When the target chamber selection mirror is oriented toward OMEGA EP, the pulse(s) are transported via SPHR9 and 10 to the backlighter OAP. An additional option is provided for the beam exiting the lower compressor to enter the target chamber via SPHR11 and 12 and reflect off the sidelighter OAP onto the target. This option provides the capability for simultaneous backlighting and sidelighting targeting. Figure 5.30 describes the configurations.

- Within the TC, the off-axis parabola (OAP) reflects the incoming beam focusing it (*f*/2.0) onto the target. The OAP is held in position by the off-axis parabola inserter/manipulator (OAPI/M), that inserts the OAP and its manipulator into the TC and aligns the OAP. A disposable debris shield (DDS) will be used to protect the OAP from target debris. The OAP, when not in use, may be housed in the OAP-Inserter (OAPI) (see Fig. 5.7).

- The target is inserted into the target chamber by the Target Positioning System (TPS). Target positioning is supported by two orthogonal Target Viewing Systems (TVS), see Chap. 7: Experimental System, S-AD-M-011.

5.2.2.2 Long-pulse beam transport

The long-pulse beam transport includes frequency conversion and transport and focusing.

- Emerging from the switchyard, the amplified long-pulse beams are directed to the FCC's where they are converted from 1053 nm (1ω) to 527 nm (2ω) in the first crystal (doubler) and then to 351 nm (3ω) in the tripler crystal.

- An uncoated diagnostic pickoff surface of the UV diagnostic beamsplitter (UV-DBS) provides a <4% sample of the frequency-converted beam to the ultraviolet diagnostics table located on the target area structure (TAS) for characterization. The UV diagnostic package (UVDP)

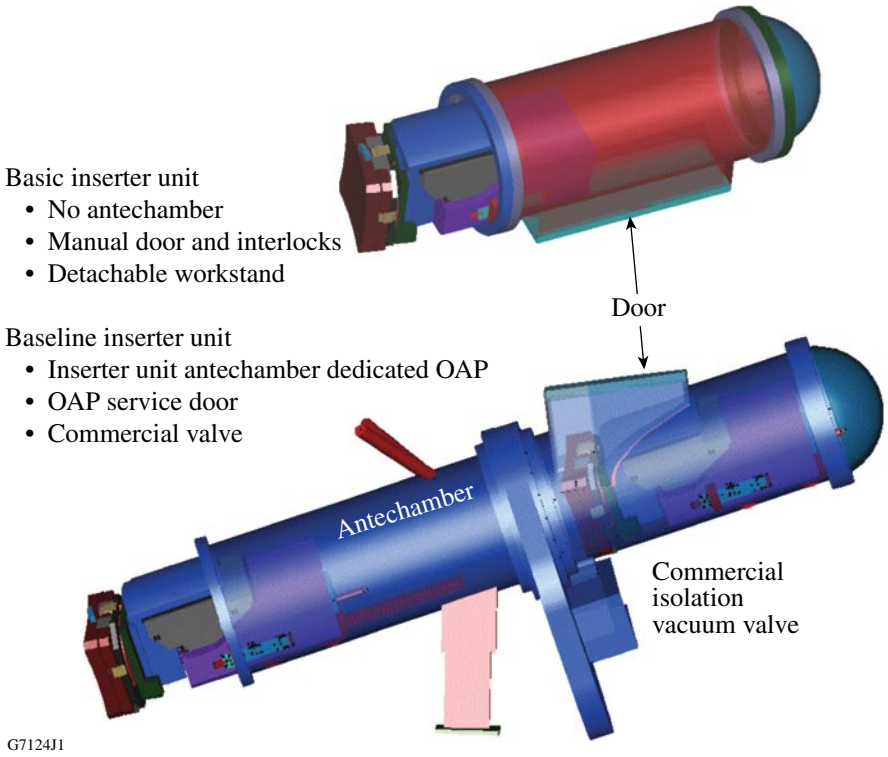

Figure 5.7
The OAPI-M's are installed on both the OMEGA EP and OMEGA target chambers. The basic inserter unit is designed without the antechamber unit, service door, and isolation vacuum valve. OMEGA EP has two basic units and OMEGA has the full-featured inserter unit.

provides a suite of diagnostics including alignment, calorimetry, harmonic energy, pulse contrast, NF and far-field (FF) imagery, and pulse shape (streak camera). (See Chap. 6: Laser Diagnostics S-AD-M-010.)

- More than 96% of the beam passes through the UV-DBS to the UV end and target mirrors. Unconverted light (1ω and 2ω) is transmitted through the end mirror and target mirror and dumped prior to the focus lens.

- The UV focus lens is mounted on the target chamber and is centered on the line of sight between the target mirror center and the target. The focus lens is a 3.4-m-focal-length, single-element, *f*/6.5 aspheric lens, with a 400-mm clear aperture. Included in the focusing optics assembly (FOA) is a blast window assembly (BWA) that consists of a vacuum window and a debris shield. The FOA is designed to accept a distributed phase plate and a distributed polarization rotator.

- The UV alignment table (UVAT) mounted on the floor of the Laser Bay just to the south of the TAS injects, in conjunction with the periscope mirror assembly (PMA), a nearly full-aperture UV alignment beam into each of the four beamlines. The UV alignment beam is injected into the main beam path before the FCC. This system co-aligns the UV alignment beam with the IR alignment beam in the UVDP. For additional information, see Chap. 6: Laser Diagnostics, S-AD-M-010.

5.2.3 Injection Subsystem

The pulse injection subsystem is located on the optical table positioned beneath the TSF pinhole assembly vacuum vessel in the Laser Bay. The subsystem takes the beam from Laser Sources and couples it to the injection fold mirror located in the pinhole vacuum vessel of the transport spatial filter. Additional beam paths to forward-going and retro-diagnostics packages as well as provision for pulse energy and spectral measurement are provided. A schematic diagram of this arrangement is shown in Fig. 5.8. One injection subsystem is required for each of the four beamlines, and the injection subsystems have only minor differences between the short-pulse (SP) and long-pulse (LP) beamlines.

The input 58.6-mm-sq beam may contain up to 12 J of IR energy.[(b)] This beam is magnified to an ~36.9-cm-sq profile that is maintained throughout the amplifier, transport, and focusing systems. To minimize nonlinear self-focusing effects, the apodizer used within the Laser Sources subsystem to create the square profile is image-relayed through the main laser system to locations near key components, including the main and booster amplifiers, the final compressor grating (G4) for short-pulse IR beams, and the frequency-conversion crystals for long-pulse UV beams. The Laser Sources beam is co-aligned with the IR alignment beam that is introduced at a beam combiner located on the IR alignment table. Beam pointing and centering into the TSF vacuum vessel is accomplished using a pair of mirrors located in front of the injection focus lens.

The injection lens focuses the beam to the Pass-1 pinhole in the TSF pinhole assembly. A window between the lower and upper injection mirrors serves as the vacuum interface for the pinhole assembly. The injection lens is a two-element telephoto lens with a focal length of approximately 3 m, and on the SP beams includes a diffractive surface that pre-corrects axial chromatic aberration. This component, together with the TSF input lens, functions as a 6.3× beam-expander telescope to achieve the ~36.9-cm-sq beam size. The beam is angularly multiplexed through the TSF (i.e., the Pass-1 and Pass-4 pinholes are horizontally displaced ~11 mm from the TSF optical axis). This arrangement ensures that the upper injection mirror does not obstruct the output beam path. The telescope relays the apodizer image to a location near the booster amplifier that is, in turn, imaged to the cavity deformable mirror plane.

Additional secondary beam paths of the injection subsystem support diagnostics for pointing/centering, energy, near field, IR spectrometer, and spatial-filter collimation. These diagnostics are located on the injection and IR alignment tables. This is discussed in more detail in Chap. 6: Laser Diagnostics, S-AD-M-010. Additional information can be found in the Laser Injection System and IR Alignment Table FDR, B-DV-M-103, Injection System Requirements, B-DT-R-001, and OMEGA EP Infrared Alignment Table Requirements, B-DV-R-001.

5.2.4 Spatial Filters

Each beamline uses a transport and a cavity spatial filter to relay the system image plane and to remove unwanted high spatial frequency noise from the amplified pulses. The TSF is located 2.5 m above the floor between the booster amplifier and the diagnostic beamsplitter and provides an internal optical table supporting the pinhole assembly and the injection fold mirror. The CSF is located between the plasma-electrode Pockels cell and the main amplifier at 1 m above the floor. An illustration of the spatial filter assemblies in the beamline is shown in Fig. 5.9 and the following sections describe their

[(b)]Injection energy is limited by the damage fluence of the injection fold mirror.

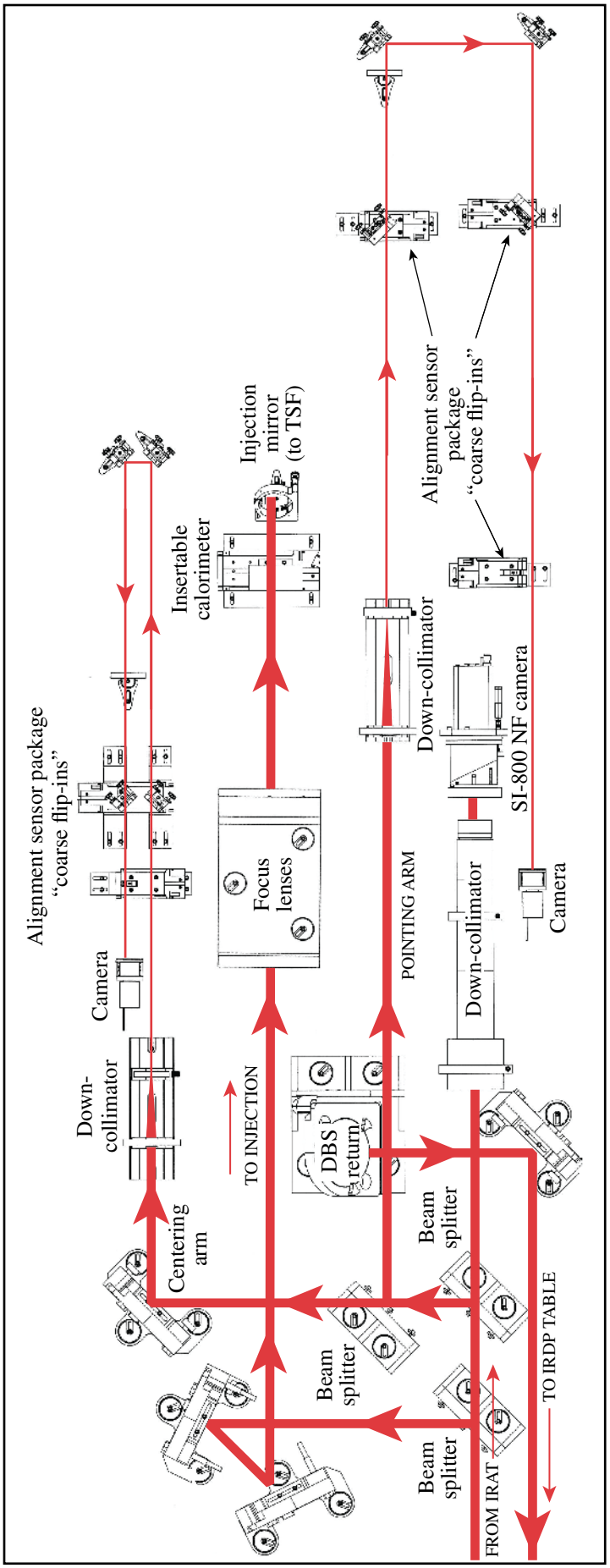

Figure 5.8
Schematic diagram of the Injection System optical table.

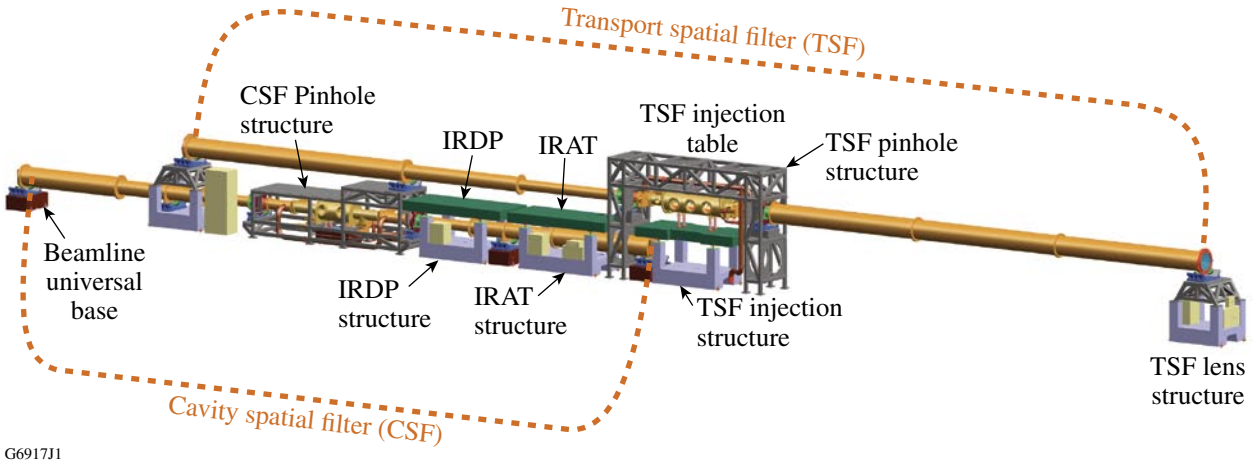

Figure 5.9
The spatial filters form an integrated system. The CSF is on the lower level between the PEPC and the main amplifier. The CSF tube is 77 ft long and weighs approximately 9000 lbs. The TSF tube on the top level between the booster amplifier and the diagnostic beamsplitter is 124.5 ft long and weighs approximately 16,000 lbs. The two pinhole structures are located in the middle of the spatial filters. Focusing lenses are near the ends of both the CSF and the TSF.

designs and functions. The spatial filters are evacuated to alleviate beam propagation effects caused by intense beams focusing in air.

The spatial filters are comprised of several subsections: the tube weldments, lenses and lens cells, variable lens spacers, structure interface package, and the pinhole manipulator. Baffles and beam dumps are also used for controlling stray light within the system. The tubes are stainless steel and rated for 5×10^{-6} Torr. The nominal operating pressure for the spatial filters is $<1 \times 10^{-4}$ Torr.

The lens cells (Fig. 5.10) are mounted on each end of the tubes. The TSF lenses are intentionally tipped 4° to divert pencil-beam reflections from re-entering the amplifiers. The resultant wavefront error caused by this offset is compensated for by the anamorphic aspheric TSF lens design. The bi-convex-

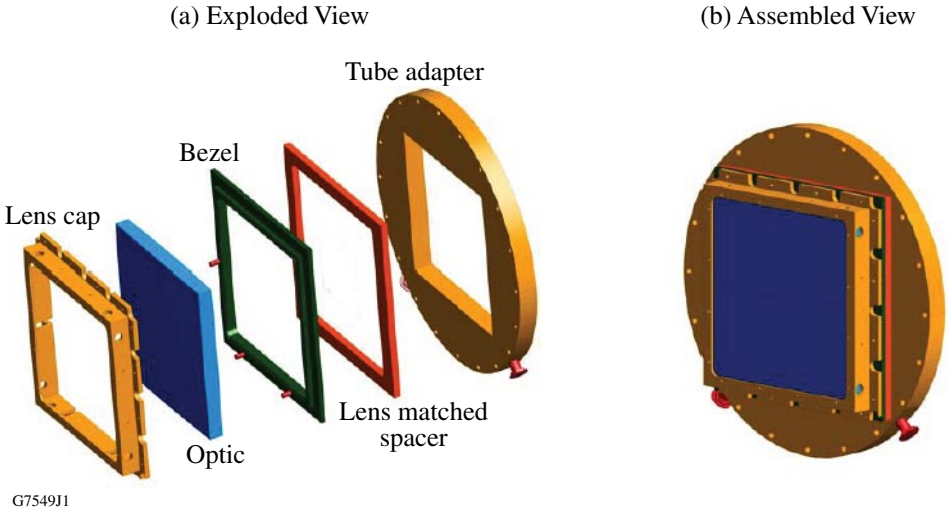

Figure 5.10
Typical spatial-filter lens cell assembly.

aspheric lenses are mounted in the cells with one side against an O ring and facing the vacuum. Simple alignment pins and screws are used to position and firmly hold the lenses centered in their mounts prior to evacuating the filters. The pinhole manipulator provides adjustments in three orthogonal axes to allow the pinhole to be correctly positioned at the focal point of the spatial-filter input lens.

The spatial-filter lenses of both the CSF and the TSF can be adjusted along the z axis to maintain collimation. Fine (±1 in.) and coarse (±6 in.) adjusters are located on both sides of each pinhole structure (Fig. 5.11).

The eight spatial filters are evacuated by a spatial-filter vacuum system illustrated in Fig. 5.12. A pair of Edwards GV600 industrial dry pumps using an EH2600 and EH2400 mechanical booster

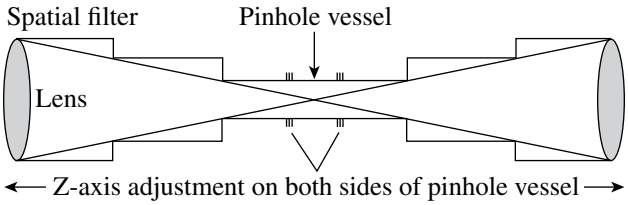

Figure 5.11
Z-axis adjustment of the spatial-filter lenses.

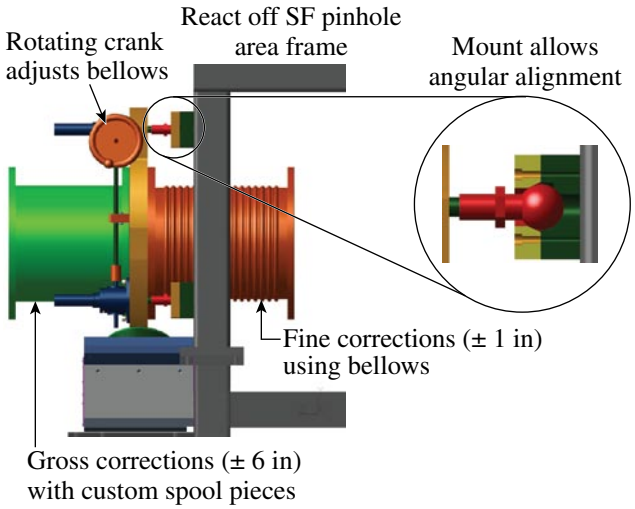

Figure 5.12
Schematic diagram of a spatial-filter vacuum system. Roughing pumps are located in the OMEGA pumphouse.

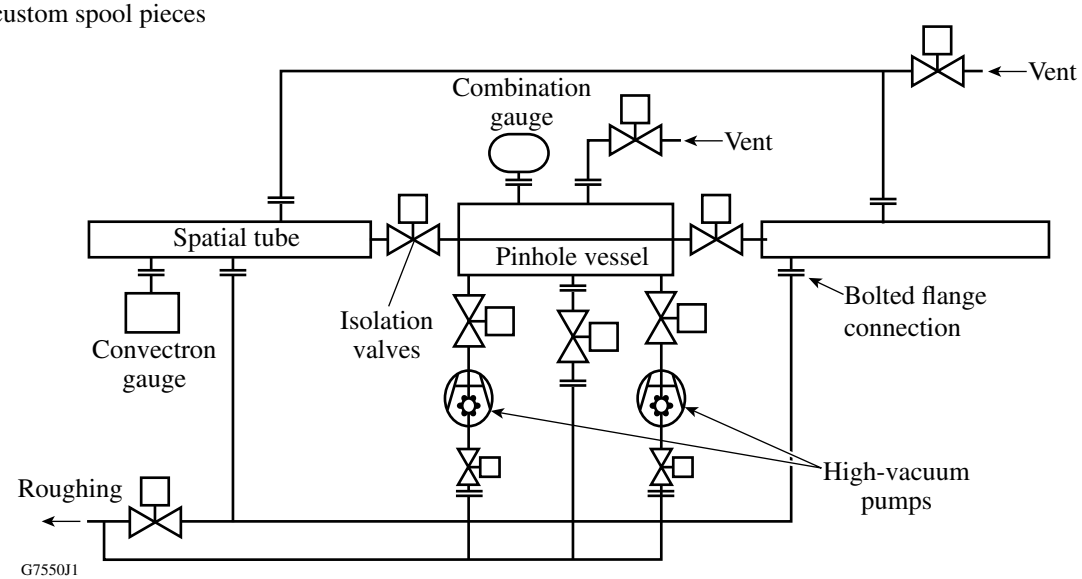

located in the OMEGA Pumphouse provide roughing vacuum (<20 mTorr). A pair of CTI Helix On-Board 10 cryogenic pumps flank the spatial-filter pinhole vessels and provides the high vacuum required for normal operations.

5.2.4.1 Transport spatial filter (TSF)

The TSF is located above the laser cavity portion of the beamline and consists of two biconvex anamorphic aspheric lenses, each having a 19-m focal length, separated by a pinhole vacuum vessel. The TSF is a unit-magnification telescope that reduces beam-intensity modulation by blocking high-spatial-frequency components of the beam at the focal plane of the lens. It also images the source apodizer to the relay planes within the beamline. The focal length, lens prescription, and axial location of the spatial filter within the laser system were chosen to maintain image-relay planes and to ensure that no lethal ghost reflections impinge upon critical laser components. The vacuum pinhole vessel houses a number of additional diagnostic and operational components located near the focal plane of the spatial filter (Fig. 5.9).

Inside the pinhole vessel a vibration-isolated table supports the injection fold mirror, a rectangular 20-mm $\times$ 35-mm optic that directs the pulse from Laser Sources through the Pass-1 pinhole. Due to the proximity of this mirror to the Pass-4 beam, the mirror is sized and located to avoid interference with the return pass. The damage fluence of the mirror represents the energy fuse in the system should any back-reflection from the target re-enter the main amplifier and propagate to the mirror.

The laser pulse passes through the TSF twice, “Pass 1” and “Pass 4”. On the first pass, the southern TSF lens collimates the beam and directs it into the booster amplifier. On Pass 4, the southern TSF lens focuses the beam with an angular offset. The angle produces a spatial offset at the pinhole plane. The deformable and cavity end mirrors are precisely tilted to steer the beam to its corresponding pinhole.

The vibration-isolated table provides a stable platform for the pinhole assembly, injection optics, and other elements near the TSF focal region. The support legs are decoupled from the vacuum tube that shifts when evacuated. The TSF pinhole plane includes three separate pairs of pinhole positions (shot, alignment, and open) and a mounting nest with a translation stage that provides for automated insertion for each position at the focal plane of the TSF lenses. The Pass-1 pinhole of the transport spatial filter is circular (washer style) and the Pass-4 pinhole has an internal conical shape. Pinholes are round and available in three sizes that accommodate three fields of view (Table 5.3). During coarse beam alignment, a flip-in alignment pinhole card made of ground glass or frosted Plexiglas is inserted into the beam path via the translation stage. The alignment card contains three alignment holes: two 4-mm holes coinciding with the Pass-1 and Pass-4 pinholes, as well as one central 4-mm hole that coincides with the mechanical and optical centerline of the TSF. A drawing of the CSF pinhole assembly is shown in Fig. 5.13.

Table 5.3: Three TSF pinhole sizes are available.

Field of view	Pinhole diameter
200 μrad	3.8 mm
300 μrad	5.7 mm
400 μrad	7.6 mm

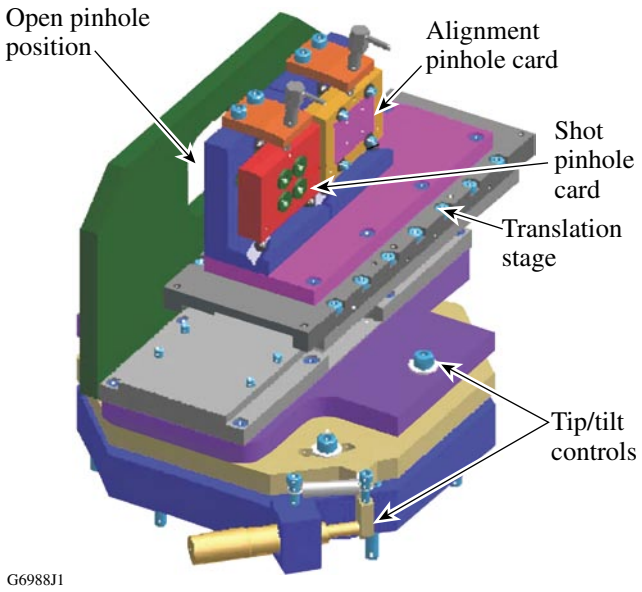

Figure 5.13
A drawing of the pinhole assembly for the CSF. The TSF pinhole assembly is similar, but has only two holes.

The pinhole vessel also supports the transport optics that provide a reference wavefront beam for the IRDP wavefront sensor (WFS). A portion of the beam emerging from the TSF is picked off by the IR-DBS and returned through the TSF to the IRDP table. An insertable single-mode fiber source located in the pinhole vessel injects light from the IRAT laser through the Pass-4 pinhole to provide the reference beam.

Beam dumps and baffles control stray reflections such as the IR DBS second-surface reflections and PEPC reflections near the pinhole plane. Beam dumps are made of stainless steel and spaced as far from the focus points as possible without overlapping the system beams. A Pass-2 beam dump absorbs the portion of light that was not properly polarized, and was subsequently reflected off of the polarizer and then propagated to the TSF pinhole region. No light may pass from the input lens to the output lens of the TSF without passing through a pinhole located at the focal plane of the input lens. Light baffles shield the entire area outside of the pinholes from any lens-to-lens light transmission. This baffling allows airflow between the center section and end sections, ensuring acceptable performance when venting or evacuating the spatial filter.

Additional information on the TSF can be found in the Transport Spatial Assembly TRD, B-DJ-R-001, Transport Spatial Filter Optical Requirements TRD, B-DJ-R-016 and the design reviews listed in Ref. 2.

5.2.4.2 Cavity spatial filter (CSF)

The CSF is a unit-magnification telescope that relays the system image plane and reduces spatial modulation by blocking high-spatial-frequency components at the focal plane of the lens. The focal length

and lens prescription were chosen to match those of the NIF laser to take advantage of the economies of scale in production. The CSF is located within the cavity portion of the beamline between the main amplifier and the PEPC and consists of two biconvex aspheric lenses each having a 11.8-m focal length separated by a vacuum vessel. It was designed using the same general requirements as the TSF but accommodates a different focal-region configuration. The relative location of the CSF in the beamline is illustrated in Fig. 5.9.

As with the TSF, multiple-pass operation with the CSF is achieved by using an angularly multiplexed beam and multiple pinholes. The angle of the beam results in a spatial offset for each pass of the laser pulse at the pinhole plane. Through proper pinhole selection and baffling, the CSF helps reduce spurious ghost reflections from reflecting forward and backward through the laser chain and causing damage and/or depleting the amplifier gain. It also isolates amplified spontaneous emission between the main and booster amplifiers.

The optomechanical components required to manipulate, condition, and align the beam(s) within the spatial filter are mounted on the vibration-isolated table in the pinhole vessel. An illustration of a pinhole assembly is shown in Fig. 5.13 (Ref. 3). Half-wave plates are used to rotate the polarization of an alignment beam and are inserted into the beam path during alignment, compensating for polarization rotation due to the PEPC firing.

Baffles in the CSF shield any lens-to-lens light transmission outside the area of the pinholes. Because of the small distance between the reflections at the pinhole plane, a single beam dump is used to absorb reflected beams from the following sources:

- portions of the beam that are not properly polarized and transmit through the cavity polarizer (POL1, Fig. 5.14) reflect off the cavity end mirror and return to the pinhole plane instead of leaving the cavity on the 4th pass as intended, and

- portions of the Pass-2 and Pass-4 beams that transmit through the CSF reflect off the PEPC surfaces and return to the pinhole plane.

Additional information on the CSF can be found in the Cavity Spatial Assembly TRD, B-DC-R-001, Cavity Spatial Filter Optical Requirements TRD, B-DC-R-016 and the design reviews listed in Ref. 2.

5.2.5 Cavity Polarizers

Brewster-angle thin-film polarizers make use of the difference between the reflectance characteristics of *s*- and *p*-polarized light for a high-reflectance coating at oblique incidence to separate the two polarizations by reflecting "*s*" and transmitting "*p*" polarization. The two polarizations are well separated at Brewster's angle, and the necessity for an antireflection coating on the second surface is eliminated. The Brewster-angle polarizer coating is based on a hafnia[(c)]/silica multilayer dielectric stack.

Each of the four beamlines contains a cavity polarizer (POL1) located in the LM2 structure between the cavity end mirror and the PEPC. This polarizer is used in conjunction with the PEPC to trap

[(c)]Hafnium dioxide (HfO_2)

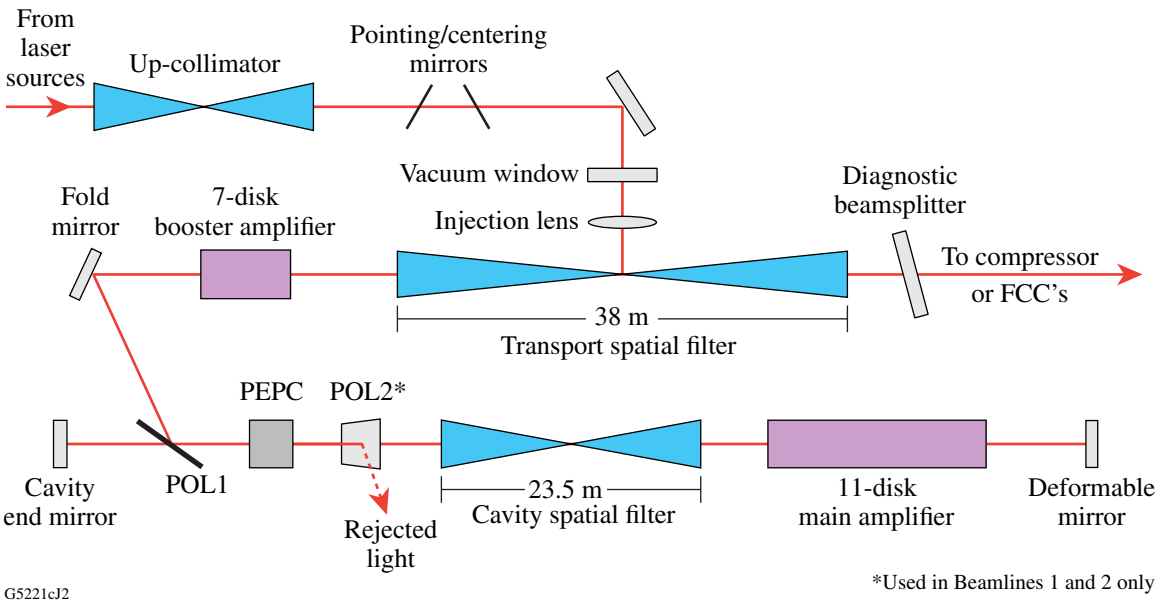

Figure 5.14
Optical components for the injection and amplification portions of an OMEGA EP beamline. The PEPC is located in the cavity between the first and second polarizers (POL1 and POL2). POL2 is used for short-pulse shots only and is not present in Beamlines 3 and 4.

the pulse in the cavity, allowing it to make a third and fourth pass of the main amplifier. Beamlines 1 and 2 also have a short-pulse polarizer pair (POL2) located between the PEPC and the CSF whose purpose is to direct retroreflection from the target to a beam dump. This pair of polarizers is set to opposing 56.4° angles, compensating for the refraction offset during beam transmission. For linear polarizers used at this angle, stringent control is required over the reflectance and transmittance of both *s* and *p* polarizations. The *p*-polarization transmittance is specified as $T_p > 0.98$ and the T_p/T_s contrast ratio as >98:1 over 8 nm of optical bandwidth in the 0% RH of a beam tube. Figure 5.15 illustrates the calculated spectral performance of such a thin-film optic.

The short-pulse polarizer assembly resides in a nitrogen-filled enclosure on a pneumatic slide so that the assembly may be inserted or retracted from the beam path. Figure 5.16 shows the assembly.

For additional information see the OMEGA-EP Short-Pulse Polarizer Assembly TRD, B-DD-R-001 and the Short-pulse Polarizer Optics Mount FDR, B-DD-M-052.

5.2.6 Plasma-Electrode Pockels Cell (PEPC)

5.2.6.1 Overview

OMEGA EP employs a multipass architecture that requires a device to switch a laser pulse in and out of the amplifier cavity. The cavity optical switch is comprised of a PEPC and a polarizer (POL1). The PEPC is located in the main amplifier cavity between the first polarizer (POL1) and the short-pulse polarizer pair (POL2) as shown in Fig. 5.14. The combination enables the beam to be trapped in the

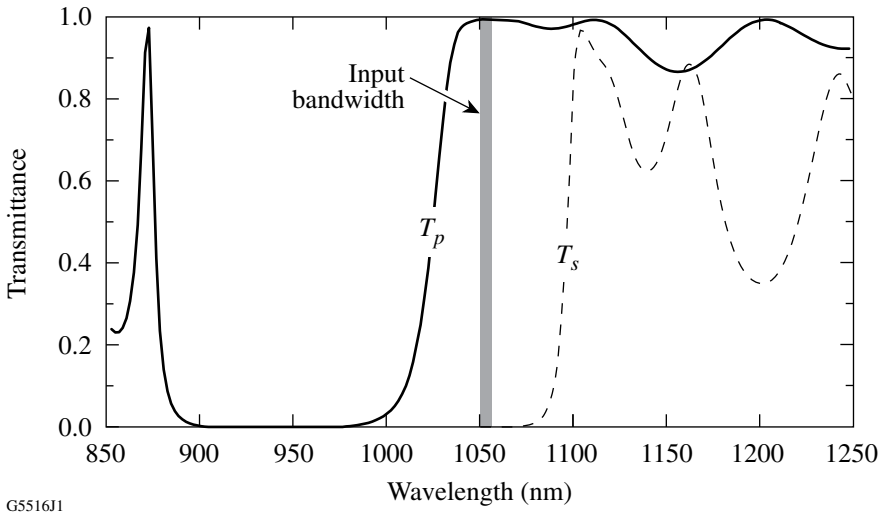

Figure 5.15
Calculated spectral performance of a thin-film polarizer coated for 56.4° incidence on a BK7 substrate and designed for operation at 1054 nm. The shaded area indicates the input bandwidth injected into the main portion of the laser.

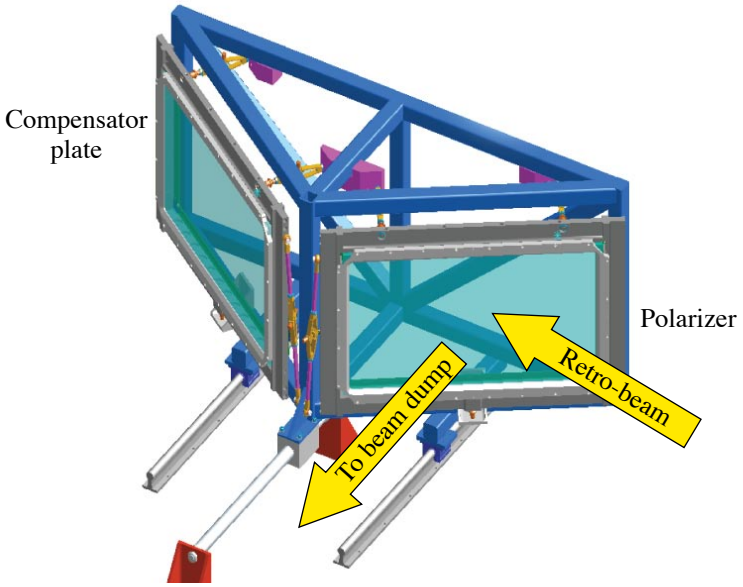

Figure 5.16
The pair of short-pulse polarizers direct target retroreflections (*s*-polarized) to a calorimeter or beam dump located on the west side of the polarizer assembly. The polarizer and its compensator are oppositely-angled to account for beam transmission offsets and are nominally positioned at Brewster's angle (±56.4°) relative to the incident pulse.

amplifier cavity between the DM and the CEM for two additional passes (one round trip), raising the gain of the system. The second polarizer, POL2, in combination with the PEPC, diverts the retroreflected beam from the target into a beam dump. Details of the PEPC system, its function, and operation follow. The original PEPC technology was developed at LLNL (Refs. 4 and 5)

The PEPC is used in short- or long-pulse system configurations and in two- or four-pass modes of operation. In four-pass mode, the PEPC is switched ON twice. The first switching event traps the pulse in the cavity, allowing it to travel back through the main amplifier, further amplifying the beam. After the beam has left the cavity, the PEPC is switched ON a second time to deflect any retroreflection from the target into a beam dump, effectively preventing it from entering the main amplifier. In long-pulse mode, where the pulse becomes frequency converted, it is not necessary to switch the PEPC ON a second time since the frequency-conversion process isolates the system from IR energy returning back from the target.

When the system is used in two-pass mode, the PEPC is "OFF" during pulse amplification and is turned "ON" after the beam has exited the cavity so that POL2 may deflect the target retroreflection into a beam dump.

For Pockels cells to rotate polarization, a half-wave voltage must be applied across the face of the potassium dihydrogen phosphate (KDP) switch crystal. In the case of the PEPC, the voltage must be applied uniformly cross the 410-cm-sq clear aperture. To apply this voltage, plasma that has minimal optical effects in transmission at 1053 nm is introduced across the face of each crystal. Each plasma stream acts as an electrode for applying voltage to the crystal.

Plasma formation uses low-pressure process gas [helium + 1% oxygen[(d)] typically at ~63 mTorr with a capability to adjust over a 10 to 90 mTorr range] on each side of the KDP crystal (Fig. 5.17). A simmer pulse begins the plasma-formation process by applying ~1.3 kV across each cell, initiating process gas ionization. The plasma pulse generators (PPG's) then discharge ~4 kV through the process gas, completing the ionization and creating the highly conductive, transparent sheets of plasma. (The current produced by the PPG's ionizes the gas, much in the way a neon sign works.) When the switch-pulse generator (SPG) is fired, the half-wave voltage (V_π ~ 18 kV) is reached, and the KDP crystal rotates the polarization of incident laser light by 90° as shown in Fig. 5.18. The SPG has a pulse width of ~300 ns, requiring precise timing with the laser pulse. In applications where it is necessary to deflect target retroreflections into the beam dump, the SPG fires twice within the same plasma pulse. Figure 5.19 shows the relationships and timing of the simmer, plasma, and switch pulses.

Protecting the amplifiers from target retroreflections requires very high contrast (>500:1). To achieve this performance, the birefringence in the cell windows caused by the pressure differential across the glass was minimized by redesigning the cell window from square to round, eliminating asymmetric stress of the corners[6] (Fig. 5.20). A contrast map of the LLE PEPC as measured on the PEPC test stand (Fig. 5.21) shows that the performance achieved 1000:1 across the entire clear aperture.

[(d)]Oxygen reacts with particles of removed graphite from the electrodes to form carbon dioxide and cleanse the system.

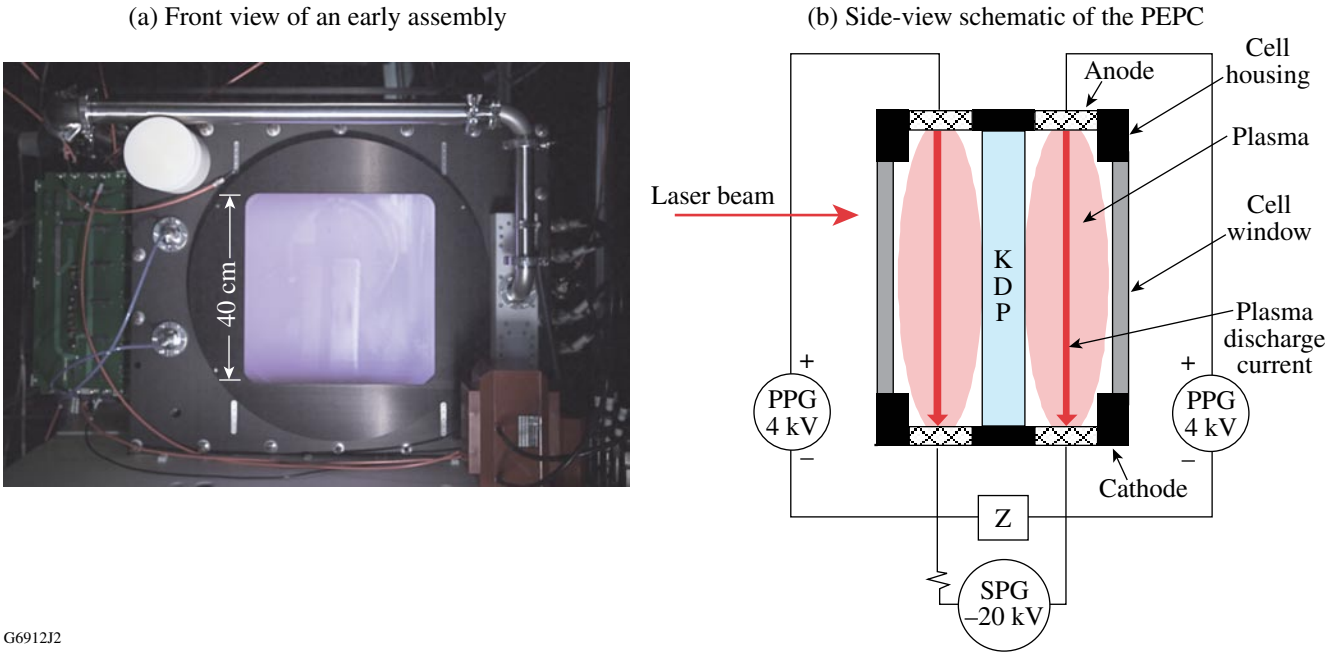

Figure 5.17
Plasma-electrode Pockels cell (PEPC). A KDP crystal is sandwiched between two evacuated regions containing He process gas. The first high-voltage electric pulse forms plasmas in the He. The second pulse (the switch pulse) applies a half-wave voltage across the KDP crystal, leading to rotation of the laser polarization by 90°.

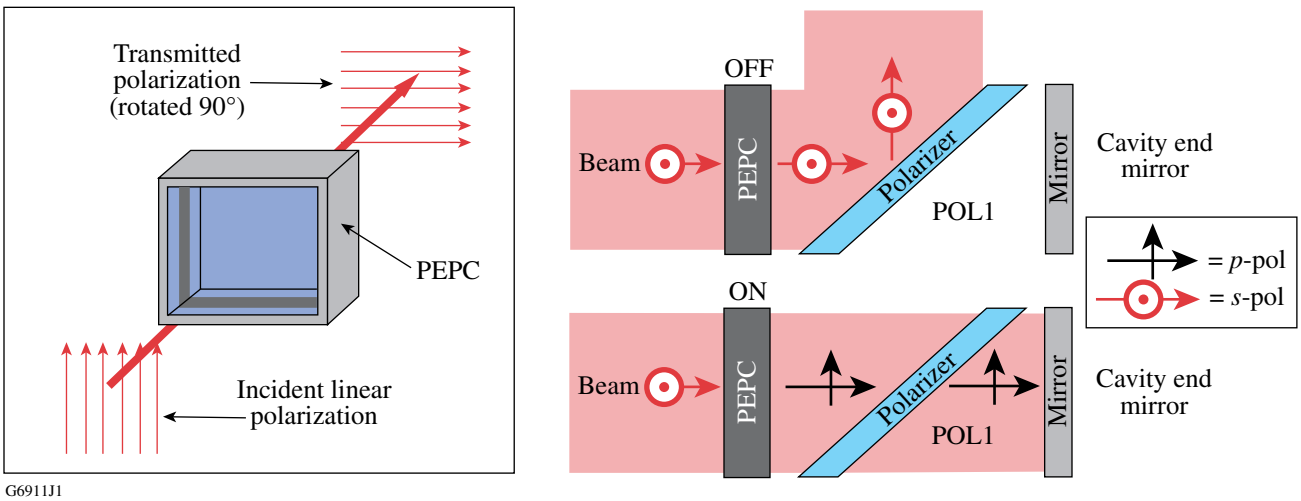

Figure 5.18
PEPC affects incident linear polarization. When the PEPC is OFF, the polarization of the light passing through the PEPC is unaltered. When voltage (~18 kV) is applied to the PEPC, the polarization is rotated by 90°. This control of polarization enables optical switching when the PEPC is used with a polarizer. Light passing through the PEPC and reflecting off POL1 is directed out of the cavity when the PEPC is OFF. When the PEPC is turned ON, light is transmitted through POL1 and on toward the cavity end mirror.

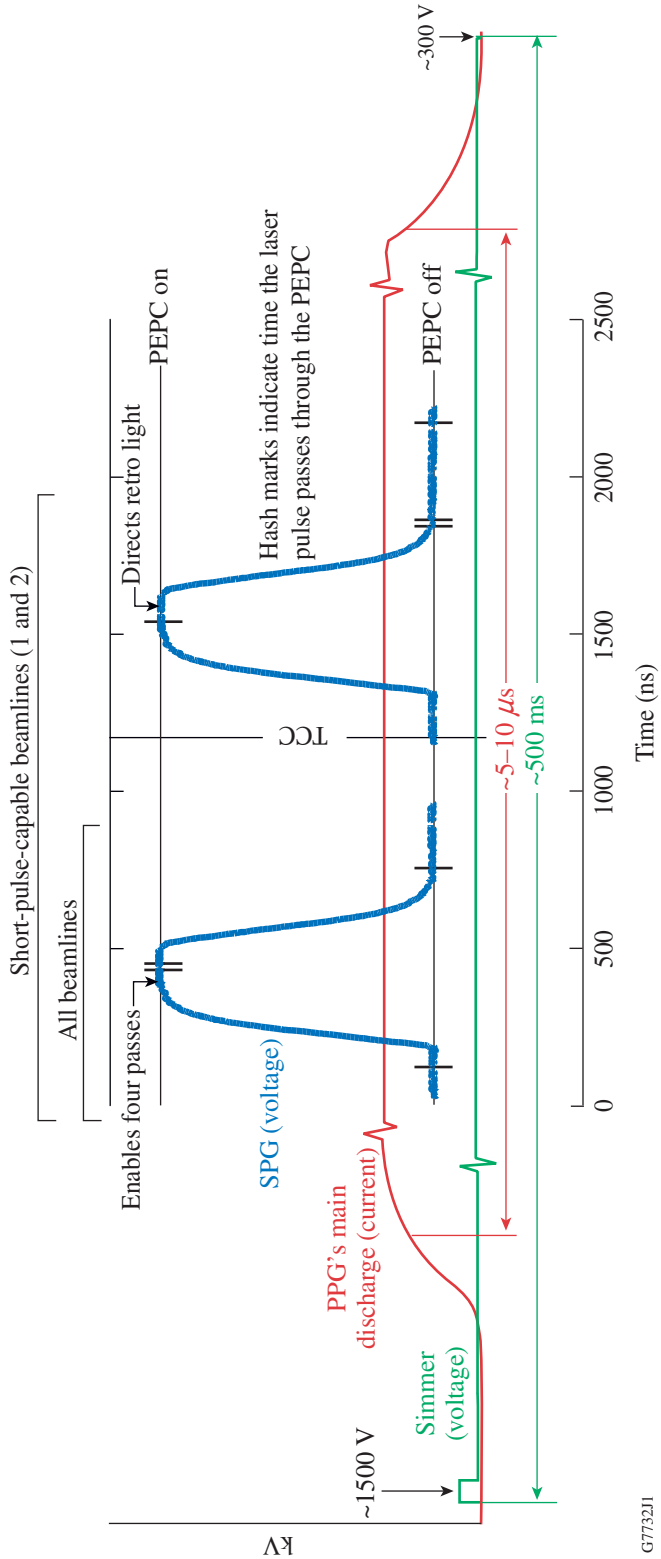

Figure 5.19
The relative timing and voltage of the simmer, SPG, and PPG pulses for the double switch pulse mode. The PEPC enables four-pass operations and prevents retroreflections from damaging optics in the amplifier. The first switch pulse occurs at approximately 400 ns and traps the beam in the cavity, forcing the beam to pass through the main amplifier four times. The PEPC turns OFF to allow the beam out of the cavity. TCC indicates the time when the pulse reaches the target chamber center. The second switch pulse diverts the target retroreflected pulse approximately 1500 ns after T–0 in four-pass operation. With the PEPC turned ON, the returning retroreflected light's polarization is rotated and reflected from POL2 toward a beam dump. Each switch pulse is ~300 ns wide. The simmer pulse begins the ionization of process gas and the plasma pulse completes the ionization process. The "PEPC-OFF-to-PEPC-ON"-SPG-voltage change is typically ~–18 kV.

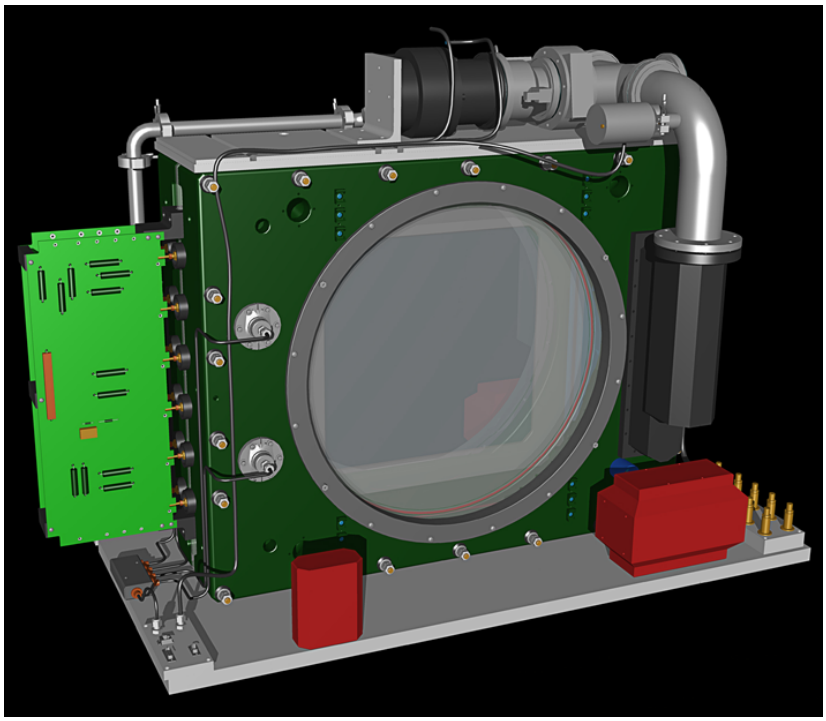

G6913J1

Figure 5.20
OMEGA EP plasma-electrode Pockels cell drawing.

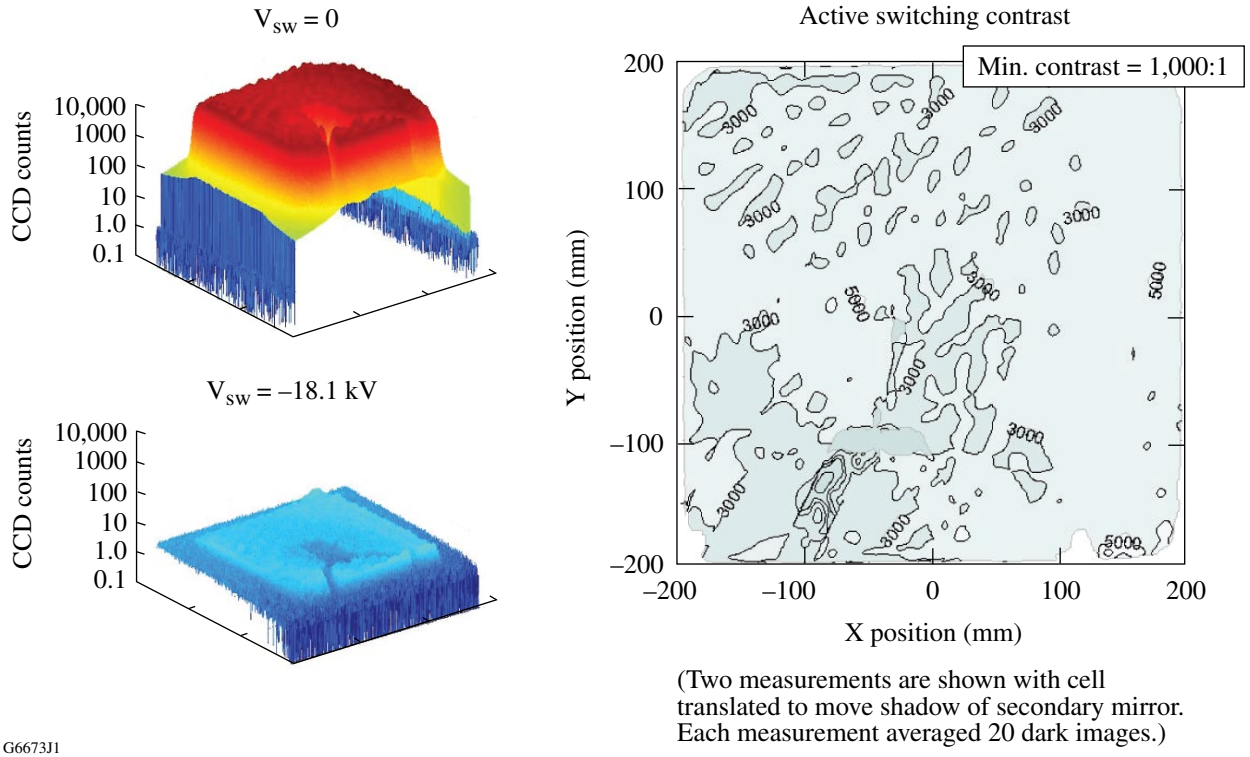

G6673J1

(Two measurements are shown with cell translated to move shadow of secondary mirror. Each measurement averaged 20 dark images.)

Figure 5.21
PEPC active contrast is >1000:1 everywhere in the clear aperture at normal incidence. Contrast is a ratio defined by the transmission of the incident linear polarization when the PEPC is OFF divided by the transmission of the incident linear polarization when the PEPC is on.

5.2.6.2 PEPC configuration

The Pockels cell is an electro-optic device that modifies the birefringence of a KDP crystal with an applied voltage. In a PEPC, the KDP crystal is bonded in a glass midplane that divides two identical low-pressure cell volumes. The cell housing serves as the structural backplane, supports the KDP mid-plane, counteracts vacuum loading of the PEPC cell windows, and defines the plasma channels [Fig. 5.17(b)].

The two halves of the cell body are machined from aluminum and anodized to provide a dielectric barrier from the plasma and consequently suppress internal arcing. A cross-sectional view of the cell is shown in Fig. 5.22. Electrically isolated anodes and cathodes are located on opposing sides of the cell, defining the plasma regions separated by the switch crystal. The anode assembly consists of a series of six oxygen-free, gold-plated, high-conductivity copper conductors (OFHC's), sandwiched between Delrin® insulators. Graphite covers on the conductors provide the electrical interface to the cell. The cathode design is more complex and includes two concentric rings of permanent magnets to help uniformly distribute the plasma in the plasma channel.

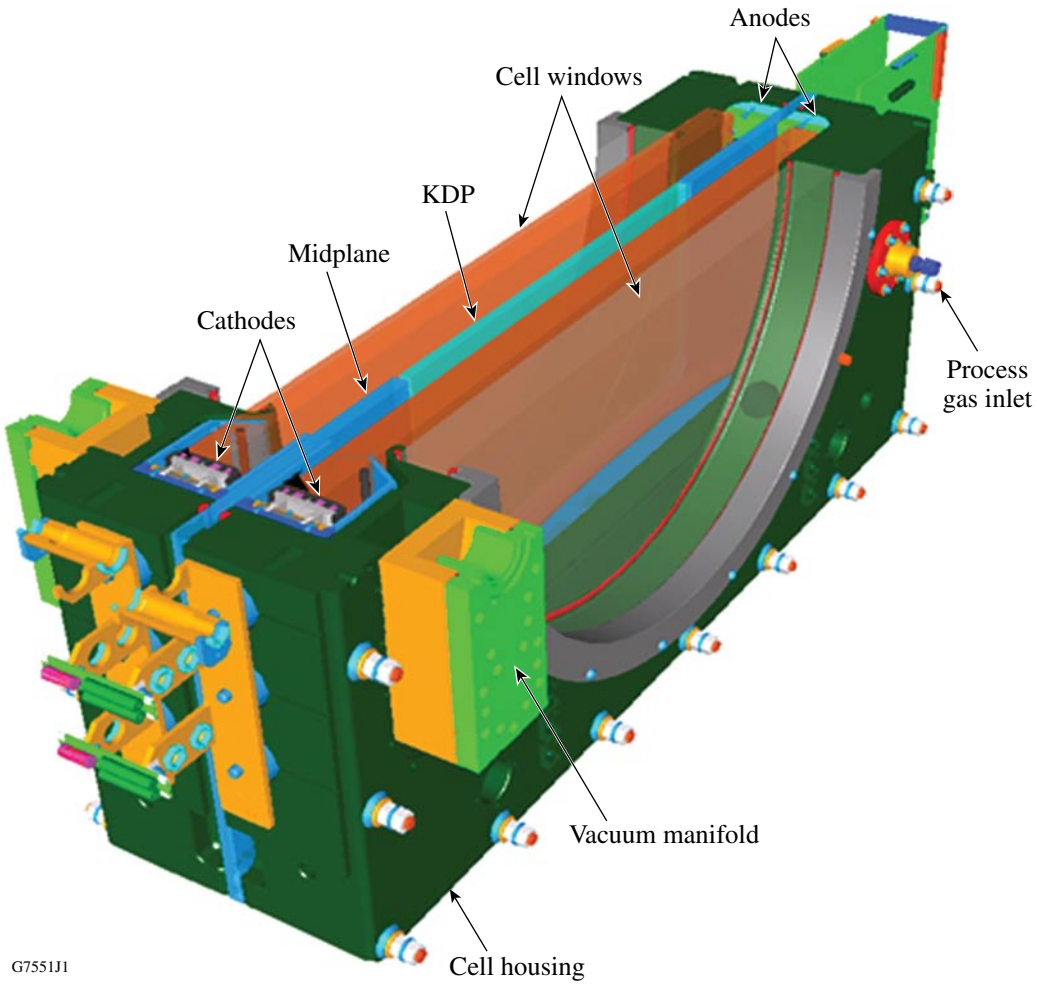

Figure 5.22
Cross-sectional view of the PEPC cell showing the midplane, switch crystal, electrodes, and vacuum attachment.

The PEPC vacuum system interfaces to the facility vacuum-roughing manifold and a turbo pump is used to maintain the cell pressure at ~60 mTorr. The process gas system provides a mixture of helium and 1% oxygen to the cell via a mass-flow controller. The oxygen converts any particles of graphite shed from the electrodes to carbon dioxide, minimizing cell contamination. The mass-flow controller and vacuum systems work in concert and are controlled by the PEPC Control System (PCS).

5.2.6.3 Pulse generators

5.2.6.3.1 Simmer and plasma pulse generator

The simmer and PPG is a low-repetition-rate, high-voltage, dual-pulse generator designed to initiate and maintain a plasma in the low-pressure gas mixture (He + 1% O_2) on each side of the KDP crystal. There are two PPG's per PEPC. A commercial gated power supply (simmer supply) initiates the gas breakdown process by delivering a relatively long (~450 ms), 1.3-kV pulse to the gas cell. After the simmer supply detects current flow (implying that the discharge has been initiated), the voltage drops to ~300 V and a steady current is maintained. A custom-designed, SCR-based, high-voltage, plasma-pulse discharge circuit superimposes a 6-kV voltage pulse to the pre-ionized gas in the cell, forming highly conductive plasma that acts as an electrode (see Fig. 5.19). The 1.6-kA pulse, delivered from a 5-μF capacitor, lasts approximately 25 μs, FWHM. For noise immunity, external trigger signals are delivered via fiber optics from the Hardware Timing System. The PPG meets the requirements given in Table 5.4.

Table 5.4: Plasma pulse generator requirements.

Parameter	Requirement
PPG pulse amplitude	6 kV±5%
PPG pulse rise time	<5 μs 10%–90%
PPG pulse width	≤15-μs FWHM
Jitter	±5 ns
PPG trigger to pulse delay	<3 μs rms

The primary hazards associated with the PPG are those presented by the high voltage. Internal voltages may reach 6 kV, with 5 kV being more typical. At 5 kV, the stored energy in the main energy storage capacitor is 63 J.

5.2.6.3.2 Switch-pulse generator

All beamlines use a solid-state switch-pulse generator (SS-SPG). Two pulses are required with an adjustable spacing between the pulses of 125 ns to 1500 ns. The SS-SPG uses inductive adder and metal-oxide semiconductor field-effect transistor (MOSFET) switches to turn OFF and ON. The PEPC test stand located in the southwest area of the Laser Bay is configured with a Thyratron-based SPG.

The SS-SPG is a low-repetition-rate, high-voltage pulse generator that serves to provide the switching pulse(s) shown in Fig. 5.19. The ensuing high-voltage pulse propagates through 200 to 600 ft of coaxial cable to the PEPC's. Rapid switching times of approximately 100 ns for the SPG are required. The pulse generated must meet stringent requirements for jitter, rise time, fall time, ripple, and repeatability. An optical trigger is supplied by the Hardware Timing System. Table 5.5 provides the SPG pulse requirements.

Table 5.5: Switch pulse generator requirements.

Parameters	Requirements
SPG pulse rise and fall time	<100 ns 10%–90%
SPG pulse width (short pulse)	>250-ns FWHM
SPG pulse width (long pulse)	>500-ns FWHM
SPG pulse flat top ripple	±5% of peak amplitude
SPG post pulse ripple	±10% of peak amplitude
Jitter	±3 ns
SPG trigger to pulse delay	<1 μs rms
SPG amplitude	<±2%

The heart of the SS-SPG is a stack of 30 magnetic-coupling pulse transformers. The primary winding of each transformer is connected to a bank of 14 energy-storage capacitors mounted on two 12-channel carrier boards. To generate a pulse, all of these capacitor banks are simultaneously discharged through their primary windings for the length of time corresponding to the desired output pulse width. At each of the 30 stack layers, the capacitor discharge current is switched ON and OFF by 28 parallel connected power MOSFET's (two MOSFET's per capacitor). There are a total of 840 power MOSFET's and 420 energy-storage capacitors in the SS-SPG.

The secondary windings of the 30 pulse transformers are connected in series with the output "stalk." This arrangement allows the SS-SPG to generate very high voltage output pulses while each capacitor and MOSFET driver is subjected to approximately 1/30th of the total pulse output potential. All 840 MOSFET's must switch ON and OFF within a few tens of nanoseconds of each other. This requires a carefully designed trigger distribution system. The SS-SPG receives a fiber-optic trigger signal, converts it to an electrical signal, and divides and distributes the signal by means of identical length cables, a series of identical drivers, and identical length circuit board traces. The duration of the input trigger signal controls the duration of the SS-SPG output pulse.

The energy-storage capacitors are connected to a high-voltage power supply. The supply output is adjustable from 0 to 1000 V dc. This voltage controls the amplitude of the SS-SPG output pulses. For a 20-kV pulse, it is set at approximately 750 V.

Each SS-SPG is housed in an electromagnetic interference (EMI) shielded electronics rack located in the south end of Capacitor Bay 2. The PEPC controllers are located in the south end of Capacitor Bay 1. The PPG's are housed in Capacitor Bay 2. The SS-SPG specifications are given in OMEGA EP PEPC Inductive Adder Solid State Pulser, Requirement Specification, C-AP-R-001, PEPC Solid-State Switch-Pulse Generator User Manual, C-AP-M-194. Additional design information can be found in the Solid-State Switch-Pulse Generator FDR, C-AP-M-099.

5.2.6.4 PEPC control system (PCS)

Each beamline has its own PEPC, which is controlled by a UNIX application on a Sun Workstation. A block diagram of the control system elements and interconnects is shown in Fig. 5.23. The software control system is described in more detail in Vol. VII, Chap. 8, S-AD-M-012. Each PCS software client of the Beamlines Executive Software coordinates the operation of and controls five major subsystems including:

1. vacuum controls for roughing, backing, turbo pumps, and valves,
2. process gas mass flow control,
3. high-voltage controls for the pulsers, including high-voltage interlocks,
4. diagnostic subsystem controls to monitor PPG and SPG voltages and waveforms, and
5. timing subsystem that provides the trigger signals to the simmer, plasma, and switch-pulse generators.

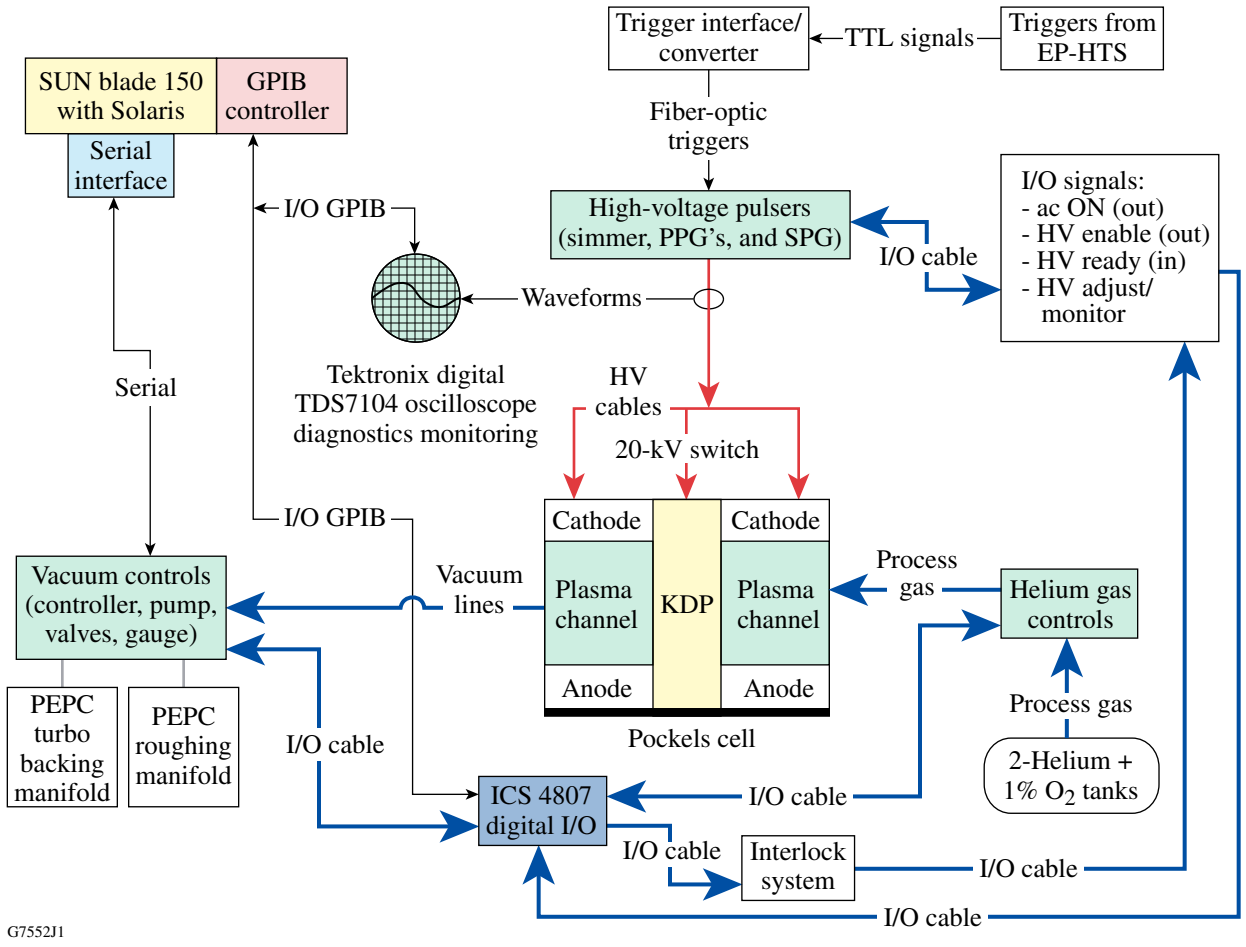

Figure 5.23
PEPC simplified control system block diagram.

5.2.6.5 PEPC timing

The Hardware Timing System (HTS) provides the precise timing needed to ensure that plasma and switch-pulse energies are triggered in coordination with the timing of the laser shot. Figure 5.24 illustrates the communication path of the trigger signals to the PEPC. The HTS rack in the Laser Sources Bay provides a 0.1-Hz clock pulse to the quad-channel delay module (QCDM). Each channel of the output pulse is converted to a fiber optic (f/o) signal (in a separate module) to provide the simmer, plasma, and two-switch pulses. The f/o triggers are sent to the PEPC control rack located at the south end of Capacitor Bay 2 where, after additional processing, they are relayed to the PPG and SPG. The simmer and plasma pulse triggers require power utility drivers (PUD's) to maintain the signals at "high" levels for the duration (~450 ms of the simmer pulses and ~25 μs for the two plasma pulses).

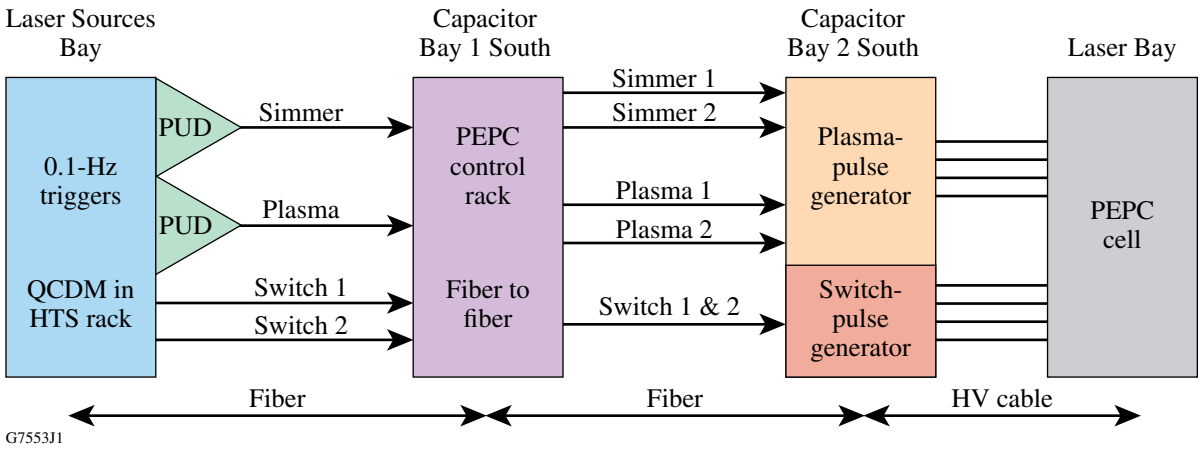

Figure 5.24
An illustration of how the triggers from the HTS are disseminated to the PEPC Control Rack, pulse generators, and finally to the PEPC cell over HV cables. An intermediate module (not shown) converts the electric signal of the QCDM to fiber optic signals.

The timing delays for the switch-pulse triggers are beamline specific and dependent on whether the laser system is operating in two- or four-pass mode. Timing delays for the simmer and plasma generators are unchanged as a function of mode of operation. The PCS determines the laser system mode from the Shot Request Form (SRF) when the PRESHOT message is received.

The PCS configuration file contains timing delays for the simmer, plasma, and both switch pulses. In two-pass mode the second switch-pulse trigger delay source configured in the quad-channel Hardware Timing System server (HTSSQ)[7] to prevent a second trigger being sent to the switch-pulse generator.

5.2.7 Wavefront Control System

The Wavefront Control System (WCS) is used with both short- and long-pulse beams to meet top-level focal-spot requirements by correcting wavefront errors. The laser system requires this adaptive optic to meet on-target intensity and repetition-rate requirements by correcting aberrations due to

- optics material and fabrication tolerance,
- laser-glass, on-shot, prompt-induced distortion,
- thermal distortions in the amplifiers from previous shots,
- alignment errors,
- gravity-induced sag in optics,
- coating-induced distortion in optics, and
- mount-induced distortion.

Adaptive optics are used to correct wavefront errors created by the optics and the laser amplifiers. These adaptive optic systems are called Wavefront Control Systems and are comprised of a DM described in Sec. 5.2.7.1 and a Shack–Hartmann wavefront sensor (SHS) described in Sec. 5.2.7.2. These devices work in concert with their control hardware and software [WCS-Coordinator, Mirror Control System (MCS) and Shack–Hartmann Sensor Service (SH-SS)] to measure and modify the laser pulse wavefront. Each of the four beamlines, both pulse compressors in the GCC, and each parabola alignment diagnostic

(PAD) has a WCS. Reference (i.e., flat) wavefronts are provided by the cw IRAT, short-pulse diagnostics package (SPDP), or PAD lasers. The architecture of the WCS is shown in Fig. 5.25.

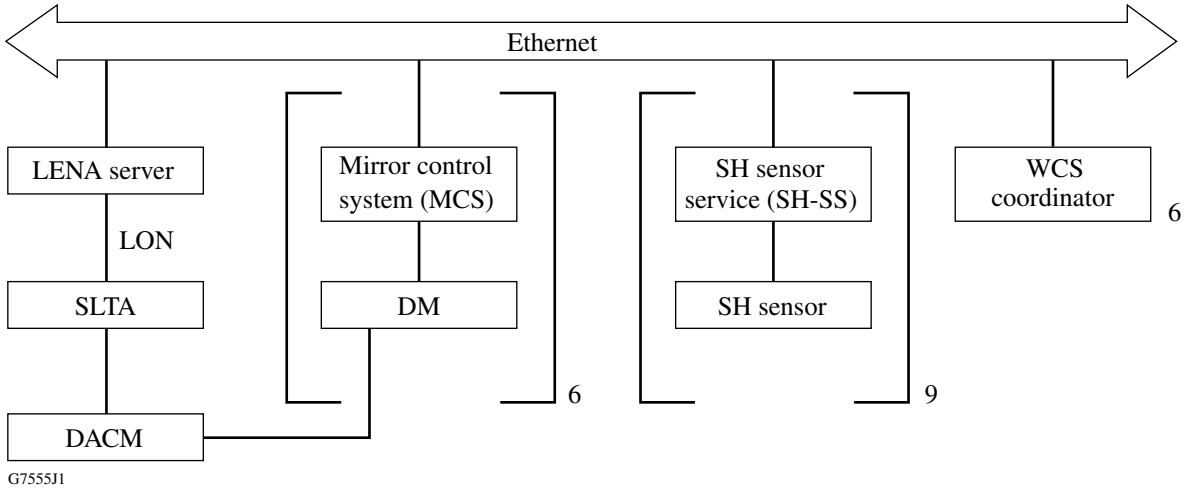

Figure 5.25
The Ethernet-based wavefront and pointing control system architecture is shown. Both the WCS and pointing control are clients of the beamlines executive software.

The beamline DM is located at the north end of the amplifier cavity and the SHS is located on the IRDP table. The DBS described in Sec. 5.2.8 reflects a fraction of light exiting the TSF back through the TSF to the SHS, where the wavefront is measured. The WCS calculates the conjugate wavefront and then deforms the DM to this shape. The wavefront of the subsequent laser pulse is thus flattened or altered to a prescribed shape, resulting in improved focusability. For simple wavefront curvatures, up to ±12 waves of correction are possible for the double-pass-reflected wavefront.

Two DM's are located in the GCC at the outputs of the upper and lower pulse compressors to compensate for residual wavefront errors associated with the optics of the short-pulse optical transport chain. Their corresponding SHS's are located on the SPDP table or in the PAD (Fig. 5.26) in the target chamber.

Each of the nine[(e)] SHS's is associated with a SH-SS that uses a charge-coupled device (CCD) (Basler) camera to acquire the incident wavefront. Each of the six DM's is associated with a MCS that controls the position of the 39 actuators upon command from the WCS Coordinator software. A WCS Coordinator manages the operation of a single WCS and is a client of the Beamlines Executive Software. The DM's are mounted on a gimbal and pointed with the balign software using servo motor actuators that tip and tilt the entire DM assembly.

The WCS Coordinator software is the core of the control system serving as the intermediary between SH-SS and MCS. It coordinates wavefront-processing algorithms, calculates voltage deviations

[(e)]There is specific software associated with each of the six DM's and each of the three PAD's.

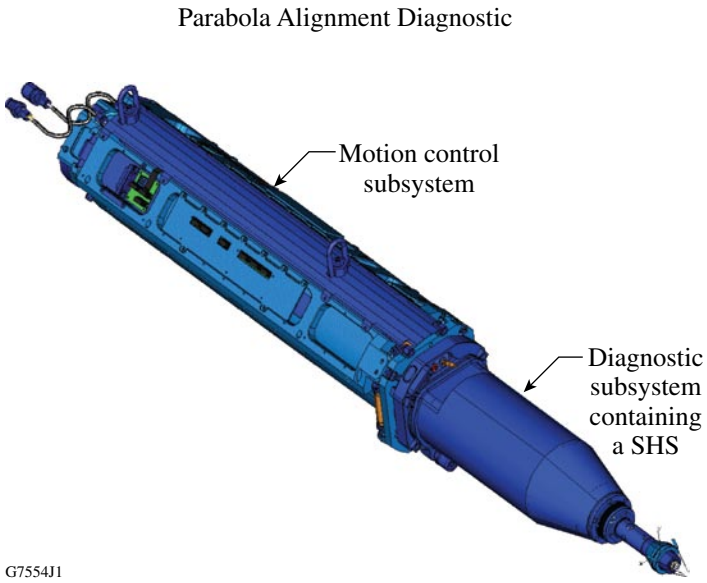

Figure 5.26
The PAD is a self-contained, TIM-based diagnostic, portable between target chambers. A Shack–Hartmann sensor measures the wavefront reflected off the OAP.

for "automated" mode of operation using the driver matrix, performs calibration algorithms, and creates driver matrices. It also monitors the wavefront in closed-loop or open-loop modes of operation and is an OMEGA intercommunications protocol (OIP) client of the WCS sub-executive.

The SH-SS provides centroids from the SHS-CCD camera to the WCS Coordinator by managing image acquisition, calculating centroids, and processing region of interest functions.

The MCS applies voltages to the DM actuators by accepting voltage deviations produced by the control algorithms in the WCS-Coordinator. The MCS applies new voltages to actuators via a Versa Module Eurocard (VME) driver and ensures that actuator voltages stay within specified tolerances.

When a DM is actively correcting the wavefront, each WCS-Coordinator is receiving wavefront information from an SHS at ~1 Hz. After wavefront processing, the MCS is provided actuator voltages deforming the mirror to the desired shape. Prior to the start of active correction, the system needs a reference wavefront and a response matrix. The reference wavefront can be a measured wavefront (from the SHS) or a calculated wavefront (from mathematical models) and is the desired wavefront at the SHS. The response matrix is a way of relating movement of a single actuator on the DM to measured responses on the wavefront sensor. Using measurements from the WFS and the driver matrix (inverse of the response matrix), the wavefront correction system can drive the wavefront measurement at the wavefront sensor to that of the reference. The system can correct for static and dynamic wavefront errors in the laser system when it is allowed to run continuously.

WCS hardware and software requirements and implementation details are described in TRD's C-AQ-R-006 and C-AQ-R-004, respectively.

5.2.7.1 Deformable mirror

The DM consists of a reaction block supporting 39 actuators that are in contact with an infrared high-reflection (IRHR) mirror whose clear aperture is 39.5 cm (Fig. 5.27). The piezoelectric actuators are symmetrically arrayed, providing a stroke of ±6 waves to compensate for simple wavefront curvatures

of up to ±12 waves when the laser system is used in four-pass mode. The spacing of the actuators limits the correction of spatial frequencies less than or equal to ~1/15 cm^{-1}. Spatial frequency improvements of a factor of ~5 (versus its uncorrected wavefront) can be achieved. In conjunction with the SHS, the DM, controlled by the WCS, is capable of continuous open- or closed-loop control of the incident wavefront at 1 Hz. During shot operations, the mirror is preconfigured to correct for previously measured laser-glass, on-shot, prompt-induced wavefront errors.


G7556J1

Figure 5.27
The photograph on the left shows the mirror and pre-epoxied actuator posts being integrated with the reaction block. The completed deformable mirror, on a gimbal mount for testing, is shown on the right.

The control rack for the four beamline DM's is located north of the DM in Beamline 2. The control rack for the DM's in the GCC is located in Diagnostic Bay 1. DM's were designed by LLNL and assembled by LLE. All six DM's are substantially the same as a standard NIF DM except for modifications made to allow operation inside the GCC in a vacuum environment. Vacuum modifications included eliminating trapped air volumes and incorporating vacuum compatible wiring harnesses.

Detailed information on the design requirements of the DM can be found in the Technical Requirement Documents: Deformable Mirror, B-DA-R-001 and Grating Compressor Deformable Mirror, B-DL-R-015.

5.2.7.2 Shack–Hartmann sensor

There is one wavefront sensor per beamline located on each IRDP table, two on the SPDP table, and one in each PAD. The WFS is comprised of a lenslet array and CCD camera. The CCD camera (Basler 102K) is connected to a frame grabber and computer using a UNIX operating system. The arrangement of lenslets maps to the layout of the DM actuator spacing. Based on 39-actuator design of the DM, the optimal number of lenslets is 77, shown in Fig. 5.28.

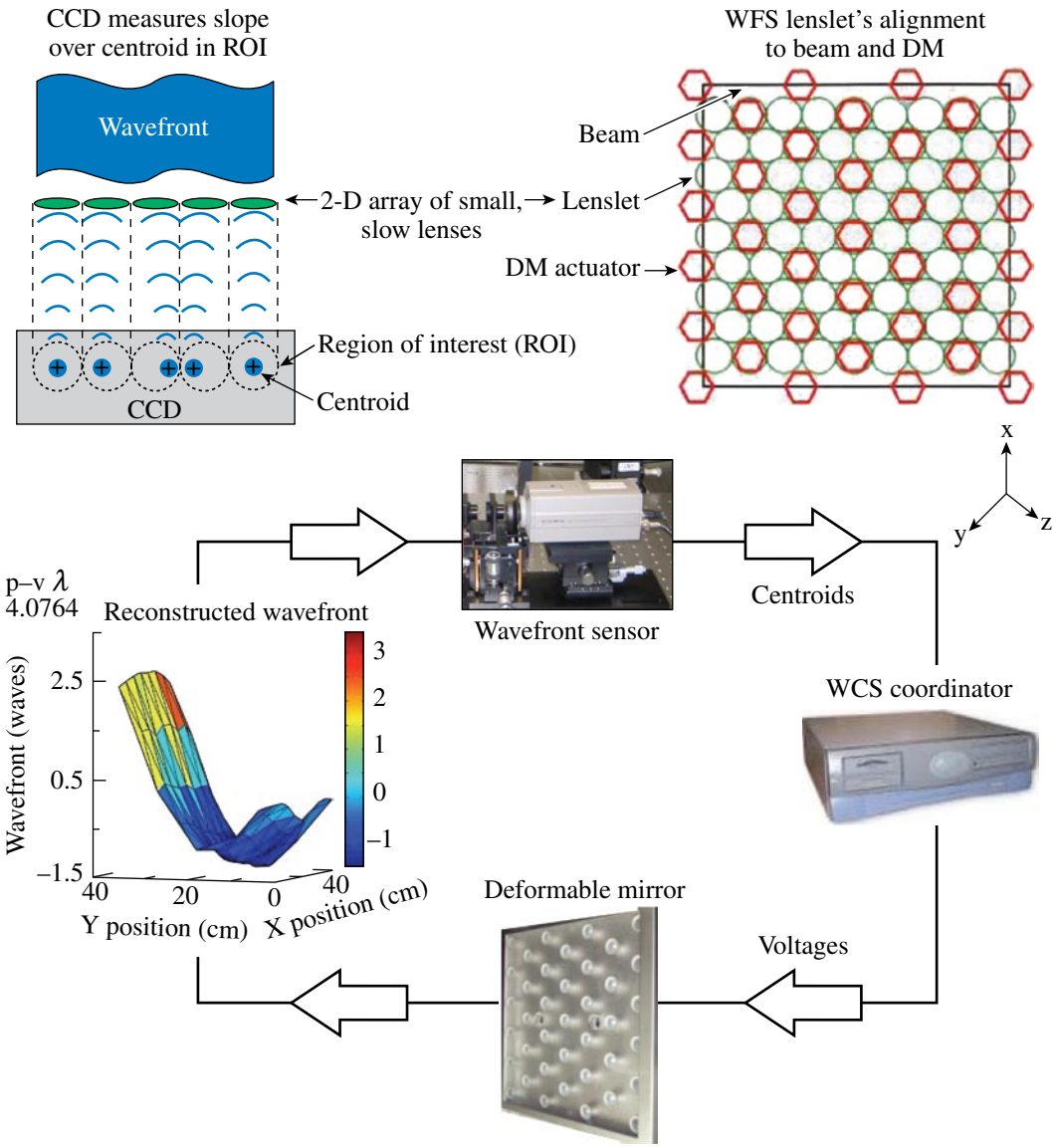

Figure 5.28
The Shack–Hartmann wavefront sensor reconstructs the input wavefront shape by measuring the local slopes at 77 points across the beam aperture. This information is sent to the WCS coordinator that calculates the delta's of these centroids from a reference wavefront array to determine a new voltage for the deformable mirror actuators. The reconstructed wavefront is then measured and adjusted again and, over a series of iterations, the wavefront is corrected. Each iteration can be completed within one second. The WCS can correct for static and dynamic wavefront errors if allowed to run continuously.

5.2.8 Diagnostic Beam Splitter

The IR-DBS is the first optic after the TSF as the main beam leaves the amplifier and before the compressor or FCC (Fig. 5.14). The light reflected from the first surface reflection of the IR-DBS propagates to the IRDP. The IR-DBS is a flat, wedged plate oriented at 0.10° relative to the beam normal and reflects approximately 0.2% of the incident light from the front surface back through the TSF output lens, where the beam is folded to fit within the TSF pinhole area vacuum vessel. Within this vessel, the beam is collimated and relayed to the IRDP table, where it is the sample beam for the various alignment and shot diagnostics.

5.2.9 Switchyard

Upon exiting the main laser, each beamline is routed to its intended path with a series of mirrors that form the IR switchyard. Short-pulse Beamlines 1 and 2 encounter a pair of mirrors in separate tower structures (Fig. 5.29) that direct each beam to the GCC (IRHR-1 and -2 in Fig. 5.30). These structures also support the full-aperture switchyard calorimeters that may be inserted into the beam path for energy measurement and calibration. The IRHR1 and IRHR2 transport mirrors may be configured to allow the beams to be sent to either the upper or lower pulse compressor. For long-pulse operation of Beamline 1 or 2, the IRHR1 mirror in each tower is removable to allow the beam to pass through to the long-pulse switchyard.

The long-pulse switchyard allows all four beamlines to be routed to the OMEGA EP target chamber. Each long-pulse switchyard consists of three IR mirrors (IRHR-4, -5 and -6) housed within structures located just prior to the frequency-conversion subsystem. To provide quadrant symmetry and equalize beam path lengths to the target chamber, the long-pulse switchyard is configured to route Beamlines 1, 2, 3, and 4 to opposing corners of a square defined by the four beamlines about the target plane, as shown in the optical model drawing in Fig. 5.31.

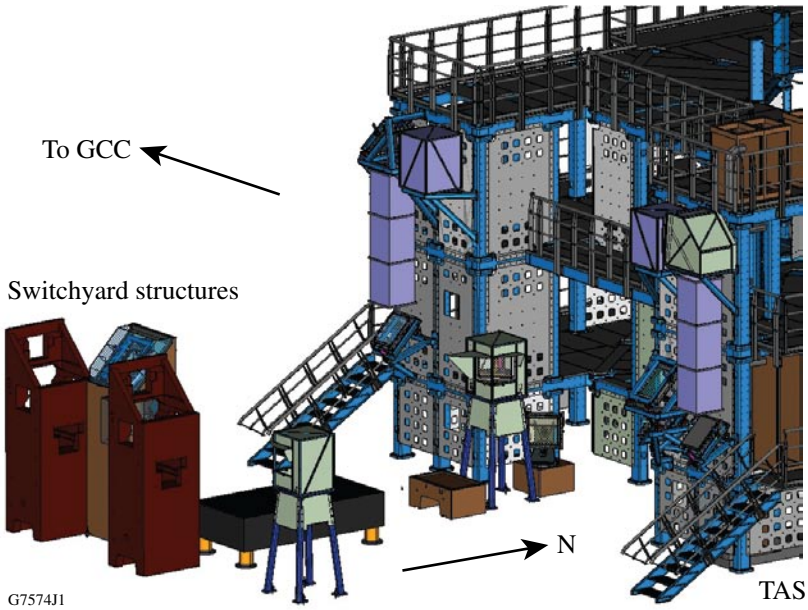

Figure 5.29
Switchyard structures route short-pulse beams from Beamlines 1 and 2 to the GCC and the long-pulse beams from Beamlines 1, 2, 3, and 4 to the TAS.

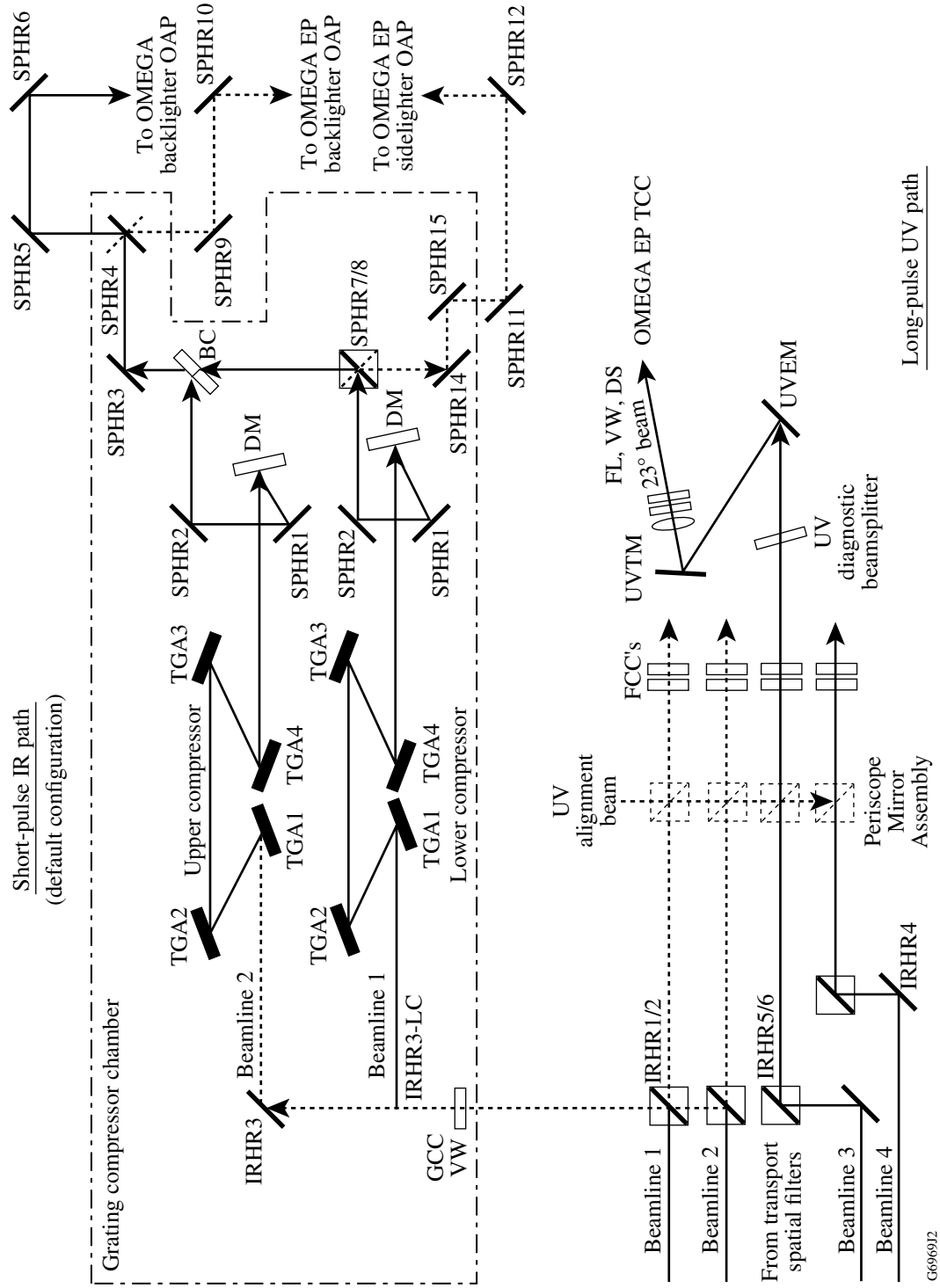

Figure 5.30
Beam transport and focusing paths are shown schematically from the transport spatial filter to the target chambers for Beamlines 1 and 2. Beamlines 3 and 4 follow the long-pulse UV path only. The short-pulse beams are IR only, and the long-pulse beams are UV only.

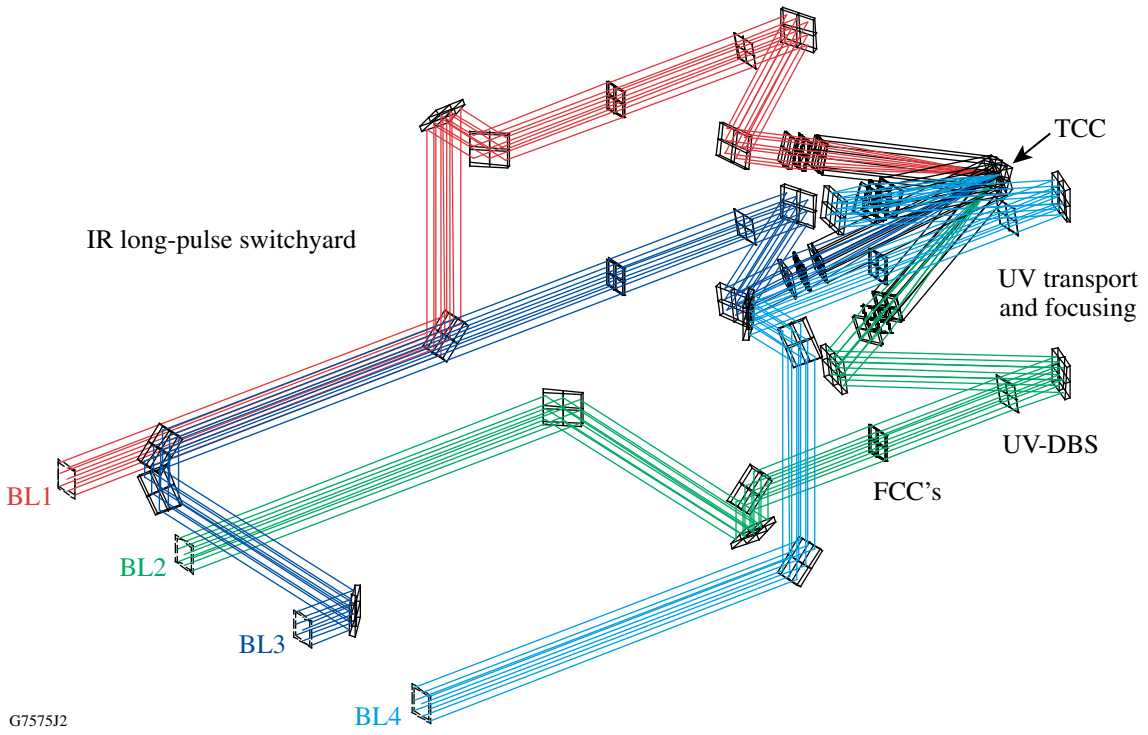

Figure 5.31
An optical model of the long-pulse transport system illustrates the relative orientations of the four beams as they enter the target chamber (not shown).

5.2.10 Short-Pulse Beam Transport

5.2.10.1 Pulse compressor design

The pulse compressor concept is based on Treacy's[8] design. This approach utilizes a dispersive delay line where the path lengths of longer wavelengths are greater than those of shorter wavelengths. The stretched and amplified pulses from Beamlines 1 and/or 2 enter the grating compressor chamber from the switchyard (see Fig. 5.5) and are reflected into either the "upper" or "lower" pulse compressor. Because of the high-power pulse, the GCC, transport tubes, and target chambers must be maintained at vacuum to prevent ionizing the air and degrading the wavefront. The two compressors have identical optical configurations through pulse compression [the second short-pulse high-reflection mirror (SPHR2) in Fig. 5.30]. Each compressor is comprised of four TGA's. Each TGA is comprised of three MLD gratings sitting on a support beam on top of a precision Newport™ rotary stage in a 1×3 array (see Fig. 5.6) that is used to align the TGA to the incoming beam or an alignment interferometer.

MLD gratings were selected because of their greater laser-damage fluence compared to other grating technologies such as gold gratings. Smaller tiles were chosen as full-aperture monolithic gratings were not available. Each tile is 43 cm high $\times$ 47 cm wide, and the width of the assembly accommodates the beam footprint given the incidence angle of 72.5° at TGA1. The gratings have a vertical line pitch of 1740 l/mm, and the outboard tiles are individually aligned to the center tile for tip, tilt, rotation, piston, and shift to a high precision, minimizing wavefront error. The diffracted beam after TGA1 propagates through the compressor, emerging after TGA4. The grating spacing and groove density between grating pairs TGA's 1 and 2 and TGA's 3 and 4 allow the 300-ps/nm stretched pulse to be temporally compressed.

The ~2.4-ns chirped[f] pulse that originates in Laser Sources has a spectrally flat bandwidth of ~8 nm; however, gain narrowing in the amplifiers reduces the bandwidth to ~3 nm. Spectral dispersion of the chirped pulse at TGA1 provides a longer path length for the red part of the spectrum than that of the blue. Thus, upon diffraction from TGA2, the red wavelengths have been delayed relative to the blue, reducing the pulse width to ~0.5 ns. This principle repeats between TGA's 3 and 4, where the red end of the pulse is further delayed and the pulse diffracting from TGA4 is further compressed. The final compressed pulse width depends on the difference between the sum of the separations between both grating pairs in the compressor and the effective grating separation in the pulse stretcher, located in Laser Sources. For example, given a pulse stretcher with a 300 ps/nm stretch ratio, a 3.3-nm bandwidth pulse at the output of the amplifiers would have a pulse width of ~1 ns. If the sum of the grating pair in the comprsesor (G1G2 + G3G4) were such that its compression ratio was ~300.5 ps/nm, then the output pulse width would be ~1.65 ps [(300.5–300) ps/nm × 3.3 nm = 1.65 ps (Fig. 5.32). Assuming each grating has a diffraction efficiency of 0.95, the intensity of the compressed pulse is increased by the ratio of the pulse widths times the diffraction efficiency, or ~1180 times prior to final focusing.

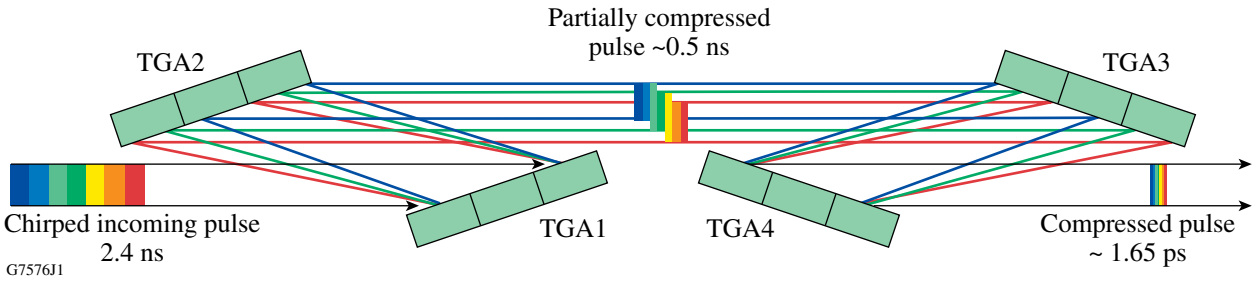

Figure 5.32
Schematic view of a pulse compressor showing the spectrally stretched incoming pulse, the four TGA's, and the compressed pulse exiting. Each TGA pair (1 and 2, 3 and 4) provides pulse compression proportional to the grating groove density and the pair spacing. Note that the spatial size of the outgoing pulse is the same as the incoming pulse. The relative spacing between TGA's 2 and 3 has no effect on pulse width.

5.2.10.2 Compressor and tiling alignment

LLE-developed alignment techniques[9] are used to achieve the coherent addition of tiled gratings. The relative grating positions and all alignment measurements are made in real-time with an interferometer whose field of view straddles the gap between two tiles. Any drift of the tiles from their aligned positions is measured by capacitive sensors and compensated via a servo loop. The tiles are pre-aligned[10] in the Tiled-Grating-Assembly Test System (TGATS) facility to have a differential piston of less than 10 μm. The center tile is fixed in position and the two outboard tiles are each aligned to it. With the servo loop engaged, an alignment precision of ±25 nm, or λ/20 p–v, is reproducibly achieved. In addition, the GCC alignment system contains two Fizeau interferometers for final tiling alignment of the upper and lower compressors *in situ*.

5.2.10.3 Compressed-pulse transport

The compressed pulse exits the compressor and reflects off the surface of a vacuum-compatible deformable mirror (identical to that used in the beamline). The DM is angled at 10° relative to the incoming pulse to direct the beam to the diagnostic beamsplitter. This splitter sends a small fraction of the beam to the SPDP table. The remainder of the pulse continues to a beam-combiner (BC) optic

[f]The wavelength of a chirped pulse changes continuously throughout the length of the pulse; typically from red to blue.

(polarizer) where the pulse from the lower compressor transmits through the BC and the pulse from the upper compressor is reflected from the surface of the BC. For the lower compressor beam, *B*-integral considerations limit the pulse width to ~80 ps for 2600-J, high-intensity shots. The temporally offset, co-aligned pulses are directed to the target chamber selection mirror (SPHR4) and finally to the OAP located in the target chamber for final focusing. The pulse from the upper or lower compressor may be directed to the "backlighter" OAP of either target chamber. In addition, the pulse from the lower compressor may be independently directed to the "sidelighter" OAP of the OMEGA EP Target Chamber.

5.2.11 Long-Pulse Beam Transport

The UV system is made up of four distinct subsystems: long-pulse switchyard, UV transport and focusing, UVAT, and UVDP. A set of IR mirrors (long-pulse switchyard) located after the main laser are used to route each beamline along the appropriate path. The UV transport and focusing system is made up of four optical subsystems: frequency conversion (see Sec. 5.2.11.1), diagnostic beam pickoff, beam transport, and beam focusing. Two additional assemblies, the UVAT and the PMA, form the subsystem that supports alignment of a UV reference source to the incoming 1ω (1053 nm) beam. A fourth subsystem, the UVDP, provides instrumentation for measurement of 3ω output-beam characteristics. Following frequency conversion, a full-aperture beam dump may be placed in the path to terminate the beam prior to reaching the UV transport mirrors.

The focusing optic assemblies (see Sec. 5.2.11.2) are mounted near the OMEGA EP target chamber such that the beams form a cone of approximately 23° half-angle with its vertex at target chamber center; the axis of the cone coincident with the focusing axis of the short-pulse backlighter's off-axis parabola. The long-pulse system provides up to 5 kJ per beamline of 3ω (351 nm) light in pulse widths from 1- to 10-ns on-target energy. This configuration allows for a variety of experimental campaigns to be carried out using x-ray backlighting. Beamlines 1 and 2 can be optionally configured to deliver long-pulse UV light to the OMEGA EP chamber. Beamlines 3 and 4 are dedicated to provide long-pulse UV beams to the OMEGA EP chamber only. The four-beamline UV layout is depicted in Figs. 5.31 and 5.33 shows a plan view. The UV transport and focusing system requirements are given in B-DR-R-005 and summarized here in Tables 5.6 and 5.7.

Table 5.6: UV input/output requirements.

Requirement	Input	Output
Wavelengths	1ω: 1053.0 nm±1.2 nm	3ω: 351.0 nm±0.4 nm (FCC output) 2ω: 526.5 nm±0.6 nm (FCC residual) 1ω: 1053.0 nm±1.2 nm (FCC residual)
Beam size	36.9 cm square (full width at 1% intensity) 35.5 cm square (FWHM intensity)	
Pulse width	1 to 10 ns	
Polarization	Linear, vertical at FCC's	Linear, vertical at UVHR1
Maximum energy	10 kJ @ 1ω	2.5 kJ @ 3ω @ 1 ns 5.0 kJ @ 3ω @ 10 ns

Table 5.7: UV focal-spot requirements.

Diameter	100 μm (80% encircled energy)
Intensity	3×10^{16} W/cm^2 @ 1 ns 6×10^{15} W/cm^2 @ 10 ns
Focusing range	±2.5 cm from target chamber center
Pointing stability	±50 μm
Pointing accuracy	±50 μm

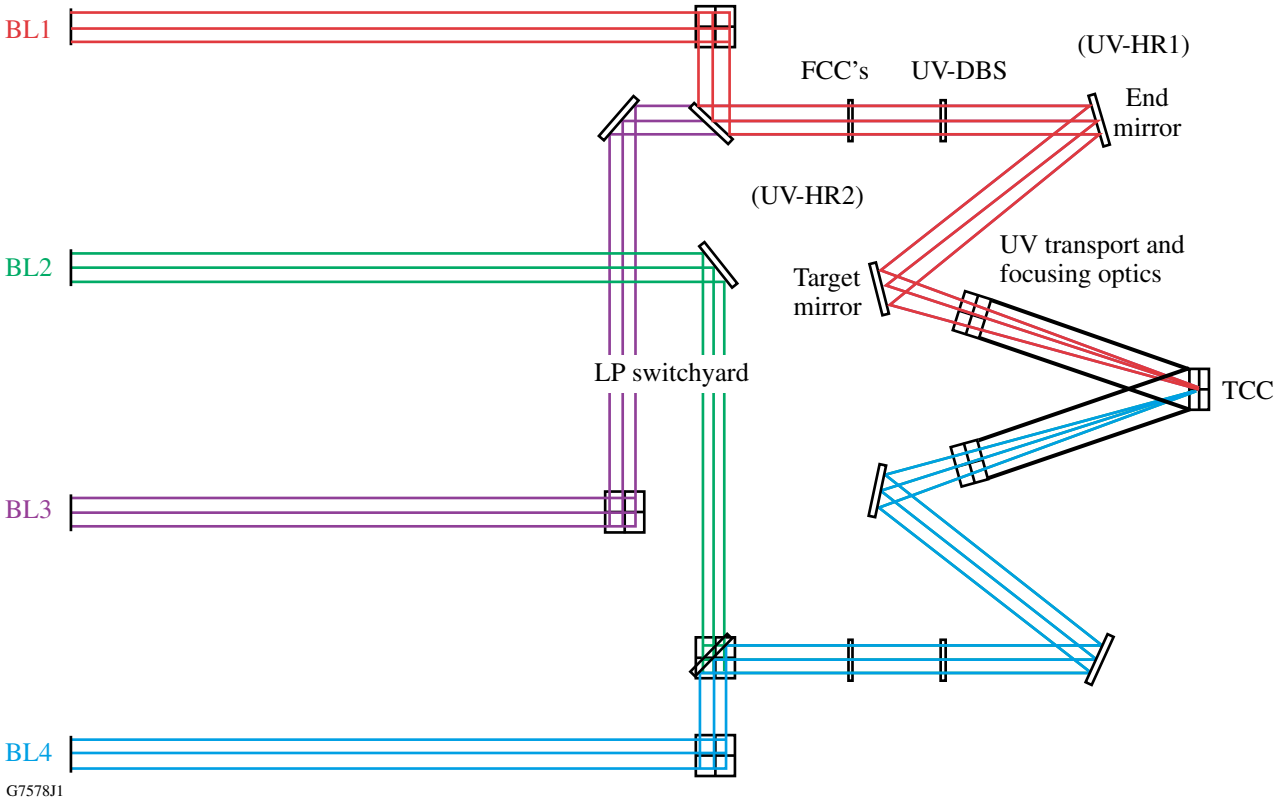

Figure 5.33
Plan view of UV transport and focusing.

Four ports are available on the OMEGA EP target chamber for UV long-pulse focusing. Four-fold symmetry is provided about a central port used for the backlighter OAPI/M, with the four ports located on a 23° half-angle cone. Each beamline has a set of two dielectric-coated, high-reflection, UV mirrors (UV end mirror UVHR1 and UV target mirror UVHR2) that are used to steer the beam to the desired target location. The mirrors are remotely controllable in tip and tilt. Each UV mirror reflects <20% IR and <20% green light, so <4% of the unconverted light is cascaded into the target chamber.

To provide quadrant-symmetry within the target chamber during short-pulse backlighting, the long-pulse switchyard is configured to route Beamlines 1 and 2 to opposite corners of the square defined by the four beamlines about the target. Figure 5.34 depicts this configuration.

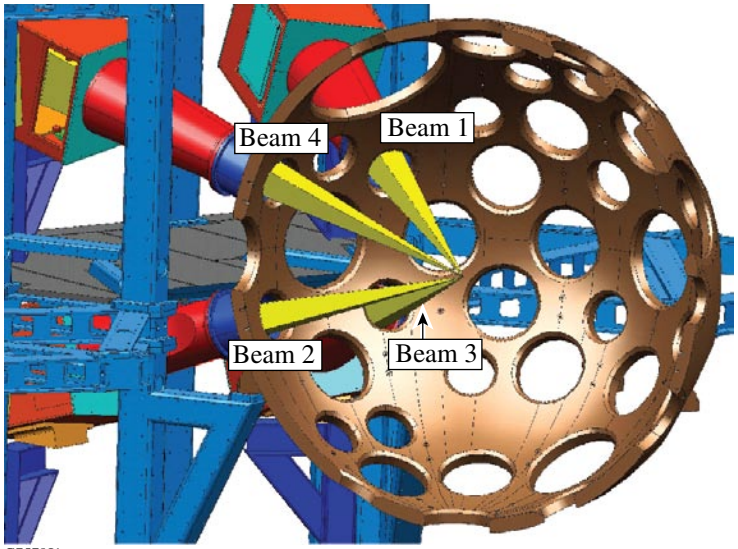

Figure 5.34
Cut-away view of the target chamber, looking from the northeast, showing the four beams coming to focus from the 23° off-axis beam spools.

5.2.11.1 Frequency-conversion system

The frequency-conversion systems are located on the south side of the TAS structure near the beam-entry points on decks 1 and 2 between the PMA and the UV end mirror (UVHR1) (see Fig. 5.30). Unlike OMEGA, the frequency-conversion system is based on type-I/type-II crystals using an angle-detuning (rotation about the O axis) configuration for the doubler. Two 40×40-cm crystals are used: an 11-mm-thick, type-I KDP doubler that converts approximately 67% of 1ω light to its second harmonic 2ω, followed by a 9-mm-thick deuterated potassium dihydrogen phosphate (KD*P) tripler[11] to mix this second harmonic with unconverted 1ω to form the third harmonic, 3ω. Compared with the type-II/type-II polarization-mismatch scheme used on OMEGA, this configuration has the advantage that a polarizer is not needed before the crystals but has the disadvantage of a tighter alignment requirement on the doubler. The choice of configuration is forced because transmission polarizers at the IR fluences of OMEGA EP are unavailable. A diagram illustrating the frequency conversion is shown in Fig. 5.35. Conceptually, the energy of three infrared (1ω) photons incident on the doubler produce a green (2ω) photon and a residual 1ω photon that, after propagation through the type-II tripler crystal, result in an ultraviolet (3ω) photon. However, some portion of residual green and infrared light is transmitted through the tripler without conversion.

The single-ray performance characteristics of the design are shown in Fig. 5.36, as calculated by *MIXER*.[12] These results are incorporated into the *RAINBOW*[13] code used to model the overall energy of the OMEGA EP system. At the highest operating IR intensities (up to 3 GW/cm^2, the limit imposed to

minimize the accumulation of B-integral in the UV portion of the system), the doubler must be detuned 350 μrad (in air) from phase matching and maintained within ±30 μrad of this peak for a conversion loss of less than 1% (±70 μrad for a loss of less than 5%). For longer pulses with IR intensity <2 GW/cm^2, the doubler is tuned to phase matching and the sensitivity to crystal misalignment or intrinsic crystal

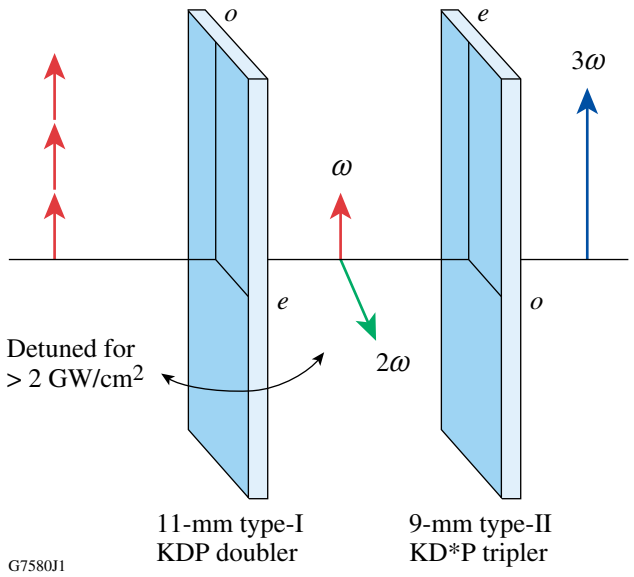

Figure 5.35
Angle-detuning scheme used for the OMEGA EP frequency-conversion system.

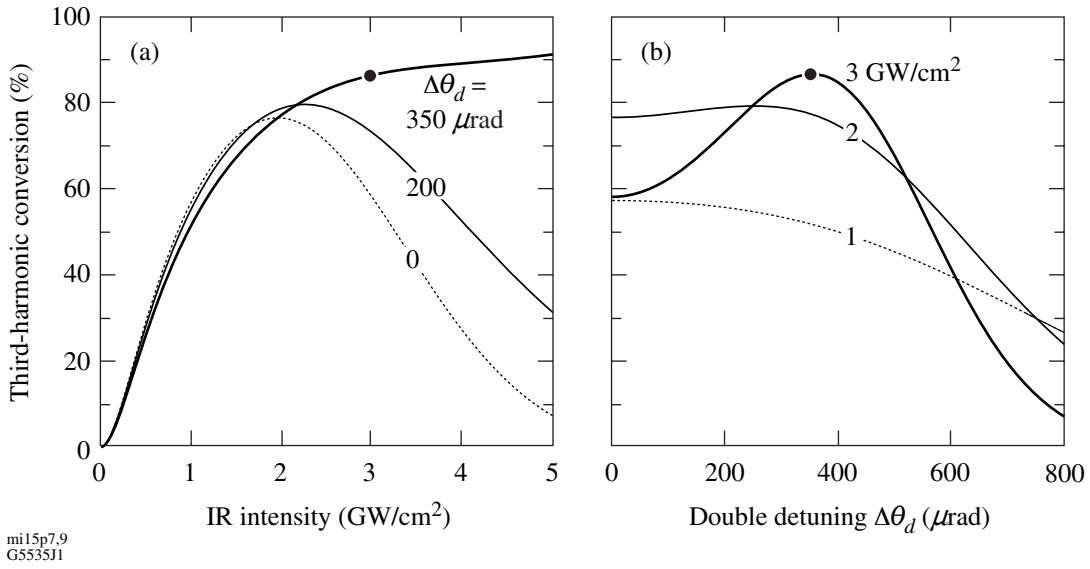

Figure 5.36
Single-ray third-harmonic–generation efficiency (a) as a function of IR input intensity for three doubler-detuning ($\Delta\theta_d$) levels measured in air and (b) as a function of doubler detuning for three intensities. The solid point indicates the highest operating IR intensity.

inhomogeneities is significantly reduced. For the angle-detuning configuration, the tripler alignment is less critical than that of the doubler. For pulse lengths below 10 ns, performance is limited by the damage threshold of the reflector coatings and not the frequency-conversion efficiency.

A dedicated control system similar to that used on OMEGA optimizes the crystal orientations, monitors the temperature, and tunes the crystals for peak UV conversion. The control system software is monitored by the Beamlines Operator in the Control Room. The KDP crystals are mounted in cells and bolted together to align their axes in a fixed orientation. The doubler is mounted such that it has a fixed wedge of 0.5° with respect to the tripler (Fig. 5.37).

Unlike OMEGA, there are no opposing beam ports in the target chamber, thus eliminating the need for a downstream UV absorption window to block retroreflected UV light. Backscattered UV light (up to 25% of the incident energy) is absorbed by the IRHR-switchyard mirrors that have been blackened by a radiological process.

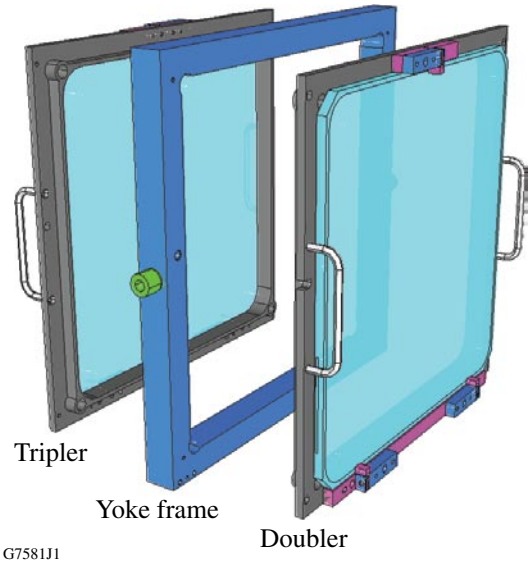

Figure 5.37
FCC assembly showing the doubler and tripler crystals mounted on their frames and separated by a yoke frame having a fixed wedge.

5.2.11.2 Focusing optics assembly (FOA)

Square, *f*/6.5, 3.4-m-focal-length, aspheric lenses[14] are used to focus the long-pulse beams[15] to the target. In the absence of aberrations, a uniform-intensity, 37-cm-sq input to the lens would produce a 6.5-μm-wide focal spot that is measured between the first minima of the far-field diffraction pattern (located at $\pm\lambda\, F/D$, where λ is the laser wavelength, F is the focal length, and D = 37 cm is the width of the beam) and contains 81.6% encircled energy. The system is specified to produce a 100-μm-diam spot in the far field. (Since a perfect 37-cm-sq beam will produce a 5.7-μm, 80% encircled energy diameter, the system is approximately 17.7 times the diffraction limit.) For most experiments, the desired spot sizes and shapes are obtained through the combination of changing the lens focal position and using an optional DPP[16] that immediately precedes the lens. These components are mounted together in a single assembly, shown in Fig. 5.38. In the vicinity of the focus lens/DPP, a distributed polarization rotator

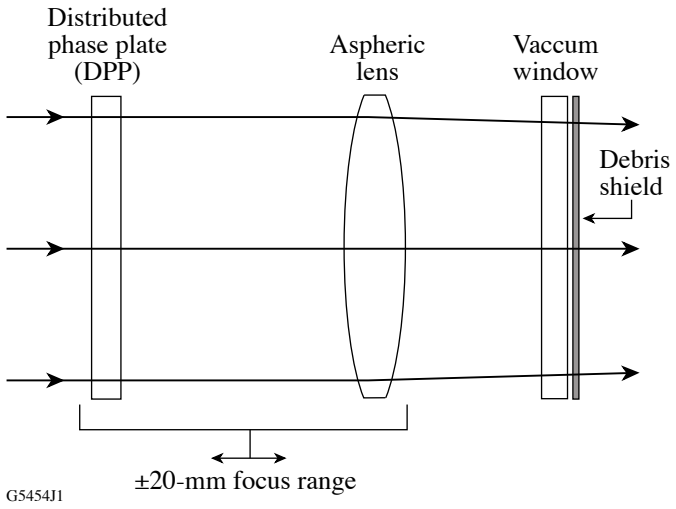

Figure 5.38
Optical layout of the focusing optics assembly (FOA) including the optional DPP. The lens and DPP move together on the inner sleeve.

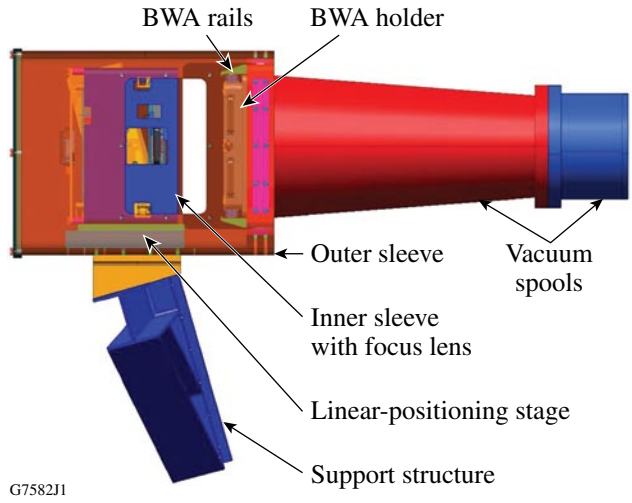

Figure 5.39
Typical of the four FOA assemblies showing the vacuum spool. The debris shield and vacuum window are designed to be removed by pulling it out of the beam path on a rail system. The FOA sits on a linear slide inserted from the left.

can be used to further improve beam uniformity on target. The assembly is mounted on a linear stage located within the outer sleeve of the focus lens assembly (Fig. 5.39).

A vacuum window[17] following the lens serves as the barrier separating the target chamber from the target bay environment, and a debris shield (DS)[18] protects the vacuum window (VW) from residual target material and debris associated with the shot. The DS and VW together are referred to as the blast window assembly (BWA) and are mounted on a removable assembly that is mounted to a spool attached to the target chamber. The focus lens and DPP are also mounted together and removed from the rear of the outer sleeve. An alignment mirror and reticle holder may be attached to the input side of the inner sleeve assembly to assist alignment.

5.3 MAJOR STRUCTURES AND VACUUM SYSTEMS

This section gives a brief overview of the structural design and installation approach and several structures are described in detail. The key structural design requirements are

- accurately located mounting surfaces for the optical components and instruments,
- micrometer and nanoradian stability within the facility's thermal and vibration environments, and
- packaging and servicing of the optical components and instruments within the constraints of the configuration.

Successful operation of the OMEGA EP system requires the stable mounting and accurate positioning of all optical components in the path from the amplifiers to the target. The concrete box beam,[g] which is the primary feature of the building structure, provides the platform for this structural stability, allowing the floor to function as a large optical table for mounting the individual support structures. Each optic is mounted to and supported by a mounting assembly that includes the fine-adjustment stages and actuators needed for routine alignment of the optic. Following the approach used on OMEGA, an intermediate "structure-to-device interface package" (SDIP) is used to adapt the optic-mounting assembly to the support structure.

Vacuum systems are provided for the spatial filters, the compression chamber, and the target chambers. Evacuated beam tubes enclose the laser-beam path between the grating compression chamber and the target chambers. Nitrogen-filled beam tubes enclose the beam path between the southern TSF lens and the DM.

The typical approach used to mount and accurately position the optical components is as follows:

(1) Structure placement is accomplished using laser-based survey techniques consisting of the Faro Laser Tracker™ and portable coordinate measurement machine (CMM), the Faro Arm™, in combination with survey monuments[h] in the Laser Bay. Each structure has multiple tooling balls attached to it at known locations from their mechanical drawings. These tooling balls and survey techniques allow for coarse placement of the structures to ±0.05 cm. Exceptions to this requirement are the main- and booster-amplifier structures that were surveyed and grouted into place to a tolerance of ±0.013 cm. The more-stringent tolerance is required to minimize beam rotation as it moves between the lower and upper portion of a beamline.

(2) The optic mounts have at least three precision tooling balls attached that serve as centering alignment fiducials. These positions are referenced in their mechanical drawings. During assembly of the mount and optic, the CMM is used to precisely measure the locations of these fiducials to within ±0.0025 cm of the position of the optic as defined on its mechanical drawing. This set of local coordinates was used to place the loaded mount onto the beamline structure's SDIP. The SDIP is then adjusted to align the clear aperture and vertex of the optic into its theoretical

[g]The concrete "box-beam" structural approach for the OMEGA EP Laser Facility provides a high degree of vibration isolation (see Chap. 9 "Facility and Safety Interlocks, S-AD-M-013).

[h]Over 30 survey monuments have been positioned in the Laser Bay. There are also six monuments located in the Laser Sources Bay. These monuments establish reference coordinates with respect to the OMEGA target chamber center.

global reference coordinate. This position is determined by the Code V® optical model (Optical Design Configuration, S-AC-G-015) (and confirmed by importing the corresponding STEP file into the mechanical system design I-DEAS™ file). Ideally, this installation step achieves coarse alignment where the optic vertex and mount monuments are located to within the measuring capability of the CMM. Once in place, conventional optical alignment techniques, such as laser bore-sighting methods are used to further align the beam. This process[19] results in a beamline ready for fine alignment.

The alignment tolerances are derived from the detailed flow-down requirements for mirror pointing presented in the pointing budget, S-AC-X-005.[20] For static beam alignment of the main laser cavity, the beam must be centered to the spatial-filter pinholes to within 5% of the pinhole radius. This translates to the pointing specification for each of the six mirrors used for operational static beam alignment to be in the 1.2 to 5-μrad range. Random vibrations and thermal drift are specified to be held to less than 583 nrad.

At each large optical component, the pulsed beam must be centered to within 0.86% of the beam width based on the centering budget, S-AC-017. This budget is based on the centered beam size on a particular optic summed with the RSS of a placement term (±3 mm) and a term associated with the 4-pass off-axis pointing through the main laser cavity (called a clear aperture hit = ±1 mm). This assures that the overall system centering is within 1% of the beam size, as shown in Table 5.8.

Table 5.8: Centering budget.

Centering Error Sources	mm	% of Beam Size
Beam to system crosshair	0.62	0.17
System crosshair to component crosshair	0.62	0.17
Component crosshair to component	0.62	0.17
Tracking error	3.16	0.86
Margin	1.6	0.43
Total (RSS)	3.7	1.00

The centering accuracy of the fine alignment view of the IRDP camera is 0.1 mm/pixel. This specification translates to >6 pixels of centering error from the desired location of the crosshairs when analyzing centering images during the operational alignment. In addition to centering, the resulting square beam profile is then oriented with its top and bottom edges horizontal to within 150 nrad (~8 to 10 pixels over the beam width).

5.3.1 Laser Bay Structures

This section gives a brief overview of the structural design approach. The beamline is a multiple-pass laser cavity that uses spatial multiplexing via an off-axis input to direct the beam through a series of pinholes located in the focal plane of two spatial-filter systems. In addition, the beamline is folded such that the optical axes of the spatial filters are situated at different centerline heights. The two centerlines are separated vertically by 1.5 m. There is also a horizontal offset between the upper and lower center lines, caused by Snell's Law displacement, due to the odd number of tilted slabs used in the booster amplifier. The four beamlines are spaced at 3-m intervals, with Beamline 1 farthest west.

The structures[21] support the optical assemblies, amplifiers, and vacuum vessels. As shown in Fig. 5.40, each beamline has been "folded" to reduce the overall length. Support structures may maintain a single or combination of support functions depending upon its location within that system. Structures used for both long- and short-pulse beams are identical except for the short-pulse polarizer (SP-POL) structure necessary for short-pulse operation in Beamlines 1 and 2.

Structures are attached to each other via their component parts and beamline enclosures. These enclosures (1) maintain an atmosphere of dry nitrogen to protect the amplifier reflectors from corrosion, (2) prevent the laser glass from surface degradation due to excess humidity, (3) provide a low-humidity environment for the polarizers to maintain a high T_p/T_s ratio,[22] free from changes in humidity, and (4) shield the sensitive optics from airborne particulate.

Each space frame and beam tube enclosure is constructed to conform to ISO Class 6 clean room specifications. All beamline structural space frames are constructed of ASTM A-500, Grade B structural steel. Some support structures are made from Zanite® (ITW Polymer Castings), a polymer composite that provides vibration damping necessary to maintain stringent pointing-accuracy requirements. After being placed and anchored, the structures are grouted to the floor using ITW Philadelphia Resins "Chockfast® Gray." Anchors used for the PEPC support and the main and cavity amplifier beams are electrically isolated from the concrete floor and inherent rebar reinforcing.

The mechanical survey began with the precise placement of 15 survey monuments in the OMEGA EP Bay. This first survey monument was placed to within ±0.3175 cm of its global reference position relative to the OMEGA target chamber center (0,0,0). Placement of this monument to within this tolerance allowed the short-pulse beam transfer tube and its mirrors to account for this offset. The remaining 14 survey monuments are installed and their locations are precisely determined using Faro Laser Tracker™. Structure, mount, and optic locations specified in the Optical Design Configuration, S-AC-G-015, were re-computed in the I-DEAS™ mechanical design package relative to the local coordinate. Structure, mount, and optic placements are based upon these derived local coordinate references.

The amplifier structures were first surveyed into position. These structures provide a fixed rail system for axial adjustment of the single-segment amplifiers (SSA's), but once grouted in place, have no transverse or vertical adjustment capability. The ends of the upper and lower structures are located to within ±0.127 cm of their absolute local coordinate position. In addition, jackscrews attached to the

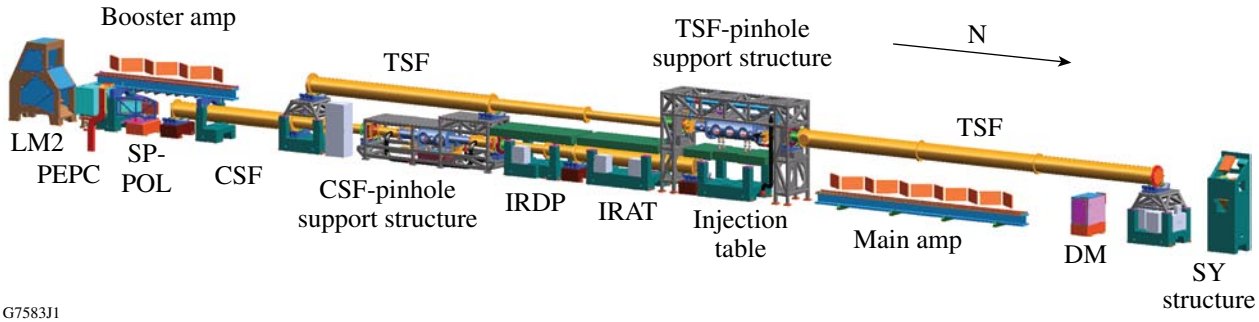

Figure 5.40
Typical beamline showing the major structures. The beam enclosures are omitted for clarity.

structures allow the structure's supporting I-beam to be leveled horizontally (across the structure) and axially (along the structure) to within ±50 μrad. The remaining structures are surveyed into place to within ±0.3175 cm.

5.3.2 Target-Area Structure and Target Chamber

The TAS is a rigid, vibration-damped support system for most of the long-pulse transport and focusing systems. The TAS supports the IR transport mirrors, FCC's, PMA, UV end and target mirrors, and the diagnostic pickoffs for the four UV diagnostic packages, as well as the diagnostic packages themselves. Short-pulse beam-transport tubes from the GCC enter the TC from the west and provide for sidelighting and backlighting target applications. The OMEGA EP target chamber[23] is similar in design to the OMEGA target chamber and has the same 3.3-m diameter. The chamber is located within the TAS[24] located at the north end of the Laser Bay. A drawing of the TAS and TC is shown in Fig. 5.41. The chamber is the heart of the experimental system, where targets are irradiated and the various diagnostics are supported. The diagnostic suite has both fixed and flexible diagnostic platforms. Transport shuttles for experimental diagnostics are provided by ten-inch manipulators (TIM's). Each provides mechanical, vacuum, and electrical/control support and positioning for any compatible instrument that needs to be positioned near the center of the target chamber.

The TC design takes advantage of the substantial infrastructure developed for the OMEGA Laser System and allows for the full compatibility of existing diagnostic instrumentation. The TC supports six TIM diagnostic shuttles, a TPS, TVS, and other support items whose designs are based on their OMEGA equivalents. The top and bottom ports are reserved for the future addition of a Planar Cryogenic Target System. The TC has two OAPI/M's that are used for the insertion and removal of the off-axis parabolas. Additional information on the TAS and TC can be found in Chap. 7, Experimental System, S-AD-M-011.

5.3.3 Grating Compression Chamber

The GCC[25] is a large rectangular vacuum chamber, 15 ft square (inside) and 70 ft long. The vessel is located in the northwest corner of the Laser Bay. It was constructed and assembled as seven individual modules joined using O rings to form the vacuum seal. The GCC and its internal supporting structures were designed to provide a stable platform for the optics in a vacuum environment equal to that of either target chamber (1×10^{-5} Torr). A mechanical decoupling scheme is provided with 28 optical-assembly support pylons that penetrate the bottom half of the compression chamber and are sealed to the compression chamber with flexible metal bellows. These pylons attach to internal structures[26] that support the optical assemblies. The internal structures are optical tables. Hard points of attachment are included for use with a trolley crane to install and remove optical component subframes. An equipment entry door on the south end facilitates insertion of large pieces of equipment, while two smaller entry doors located on the north and south ends provide personnel access and ventilation. A rendering of the GCC is shown in Fig. 5.42.

The GCC houses two independent pulse compressors, deformable mirrors, compressor alignment mirrors (CAM's), transport mirrors, full-aperture calorimeters, a beam combiner, and the transport chain optics to the SPDP table. A diagram of the internal components of the GCC illustrating the 14 optical tables, 8 TGA's, and target chamber selection mirror is shown in Fig. 5.4.

(a) TAS consists of three elevated levels above the laser bay floor

(b) First level deck cutaway view

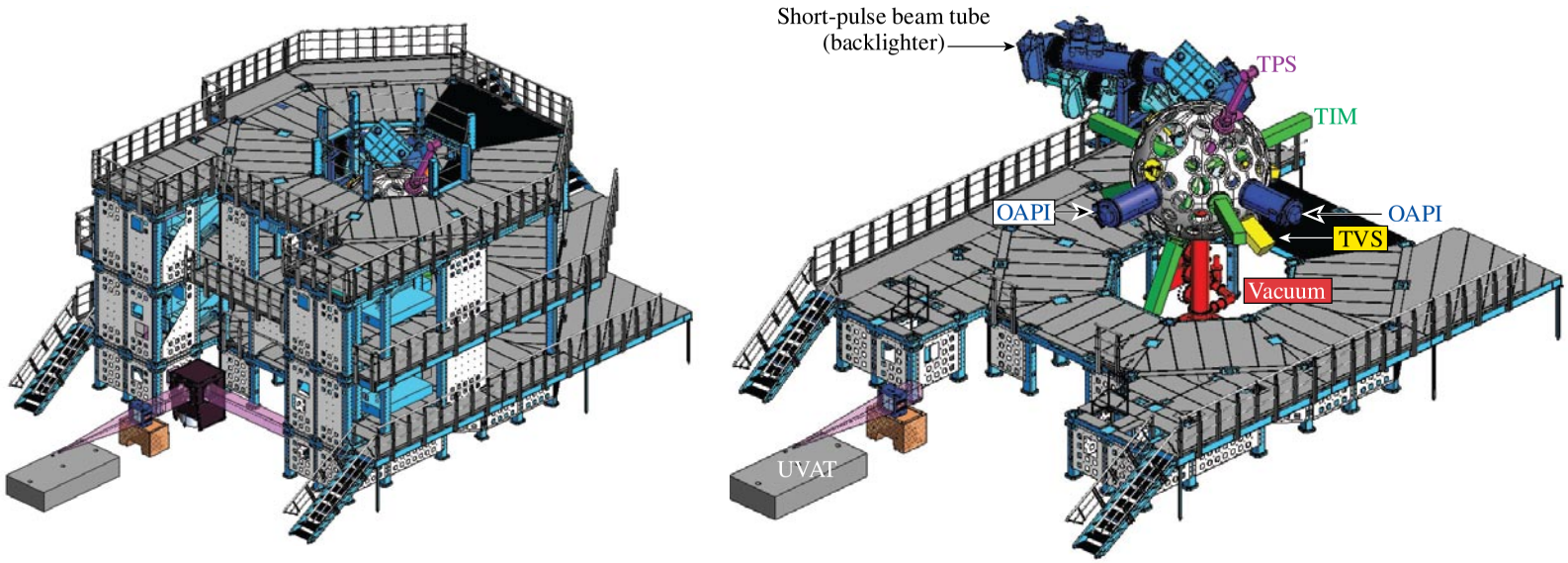

(c) Second level deck cutaway view

(d) The four-long-pulse beams and UVDP/UVAT tables

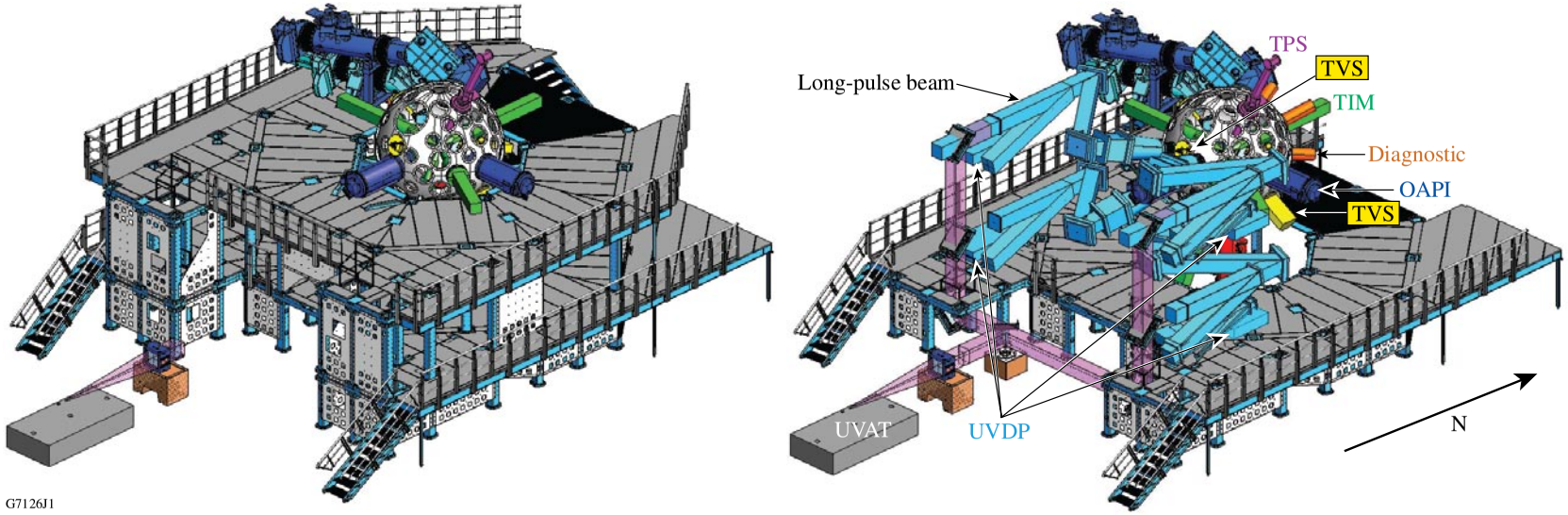

Figure 5.41
The TAS consists of three levels (a) above the laser bay floor. The first-level deck cutaway view (b) shows the target chamber and some of its devices. The second-level deck provides access to the OAPI's and three of the TIM's (c). The four long-pulse beams occupy a substantial volume on the SE and SW towers (d). The UVAT is on the floor south of the TAS.

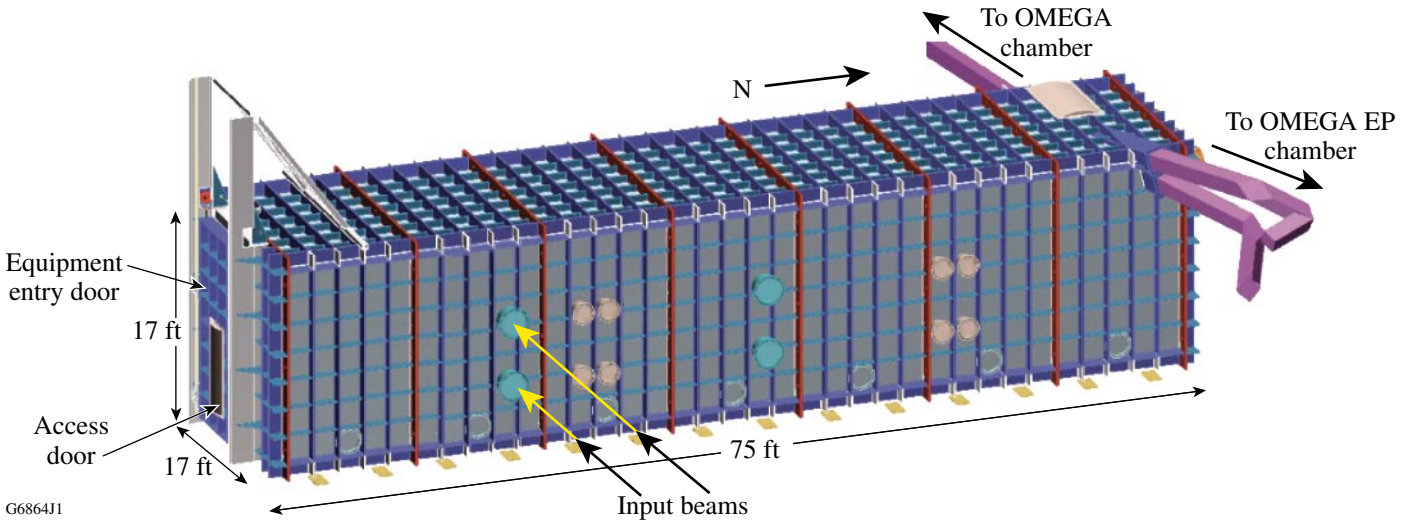

Figure 5.42
A drawing of the GCC shows the main equipment access door to the south and the beam exit ports to the north. The two beam exits to the east support OMEGA EP's sidelighter and backlighter capabilities. The west beam penetrates the shield walls of OMEGA EP and OMEGA and enters the OMEGA target chamber at port H9.

5.3.4 Vacuum Systems and Beamline Enclosures

The OMEGA EP rough vacuum system[27] provides continuous operation at a vacuum of $\leq 2 \times 10^{-2}$ Torr to the following major vacuum systems:

- Grating compressor chamber and spatial filter assemblies
- Target chamber auxiliary roughing manifold
- Target chamber turbopump backing manifold
- Cryogenic Handling Target System vacuum manifold
- PEPC turbopump backing manifold
- PEPC turbopump roughing manifold

The roughing pumps are centralized in the "OMEGA Pumphouse." In addition to the pumping capabilities, instrumentation monitors the vacuum environment of each vessel. Additional pumping capacity is provided to allow for the maintenance or failure of any one roughing pump without interrupting service. Venting of each manifold is accomplished with filtered room air at the end of the vacuum line. The vacuum pumps connect to the client vessels via a network of 304L stainless steel manifolds and pipes.[28] Two networks were implemented, one providing ~600-standard cubic feet per minute (SCFM) capability utilizing Edwards GV160 pumps and one providing ~2000-SCFM capability utilizing Edwards GV600 pumps. Each is a dry pump and uses a mechanical booster to increase pumping efficiency.

Manifolds that connect the pumps to each pipe network allow each pump to connect to any pipeline in that network.[29] Component sizing and quantity were dictated by achieving the necessary requirements for pump-down times as noted in Table 5.9. Actual pump down times may be longer.

The vacuum controls are a distributed input/output (I/O), programmable logic controller (PLC)-based system using GE Fanuc Series 90-30 technology. The backbone of the system is the LLE Ethernet and the HMI (Human Machine Interface) based upon the HMI/SCADA (Supervisory Control and Data

Table 5.9: Vacuum chamber volumes and estimated pump down times.

Vessel	Estimated Vessel Volume (liters)	Estimated Pump-down Time (minutes)	Minimum Operating Pressure (Torr)
GCC	446,000	90	$\leq 1 \times 10^{-4}$
Target Chamber	16,000	5	$\leq 1 \times 10^{-4}$
Transport arm to OMEGA TC	2,000	5	$\leq 1 \times 10^{-4}$
Transport arm to OMEGA EP backlighter	1,500	5	$\leq 1 \times 10^{-4}$
Transport arm to OMEGA EP sidelighter	1,800	5	$\leq 1 \times 10^{-4}$
TSF vessel (each)	8,500	10	$\leq 6 \times 10^{-4}$
CSF vessel (each)	4,113	15	$\leq 6 \times 10^{-4}$

Acquisition) software. The four major independent software vacuum controllers include the pumphouse, the spatial filters, the GCC and transport arms, and the target chamber, and each subsystem has its own Cimplicity® Graphical User Interface (GUI). Each instance is an OIP client of the appropriate Executive. Details of the pumphouse, short-pulse, and target chamber clients are discussed in Volume VII, Chap. 7, Experimental Systems, S-AD-M-011.

Pumphouse controls[30] monitor the status of each roughing pump and that of each dedicated vacuum line. The GUI shown in Fig. 5.43 is available in the OMEGA Pumphouse and the OMEGA EP Control Room at the experimental operator's console and controls the main and auxiliary roughing systems.

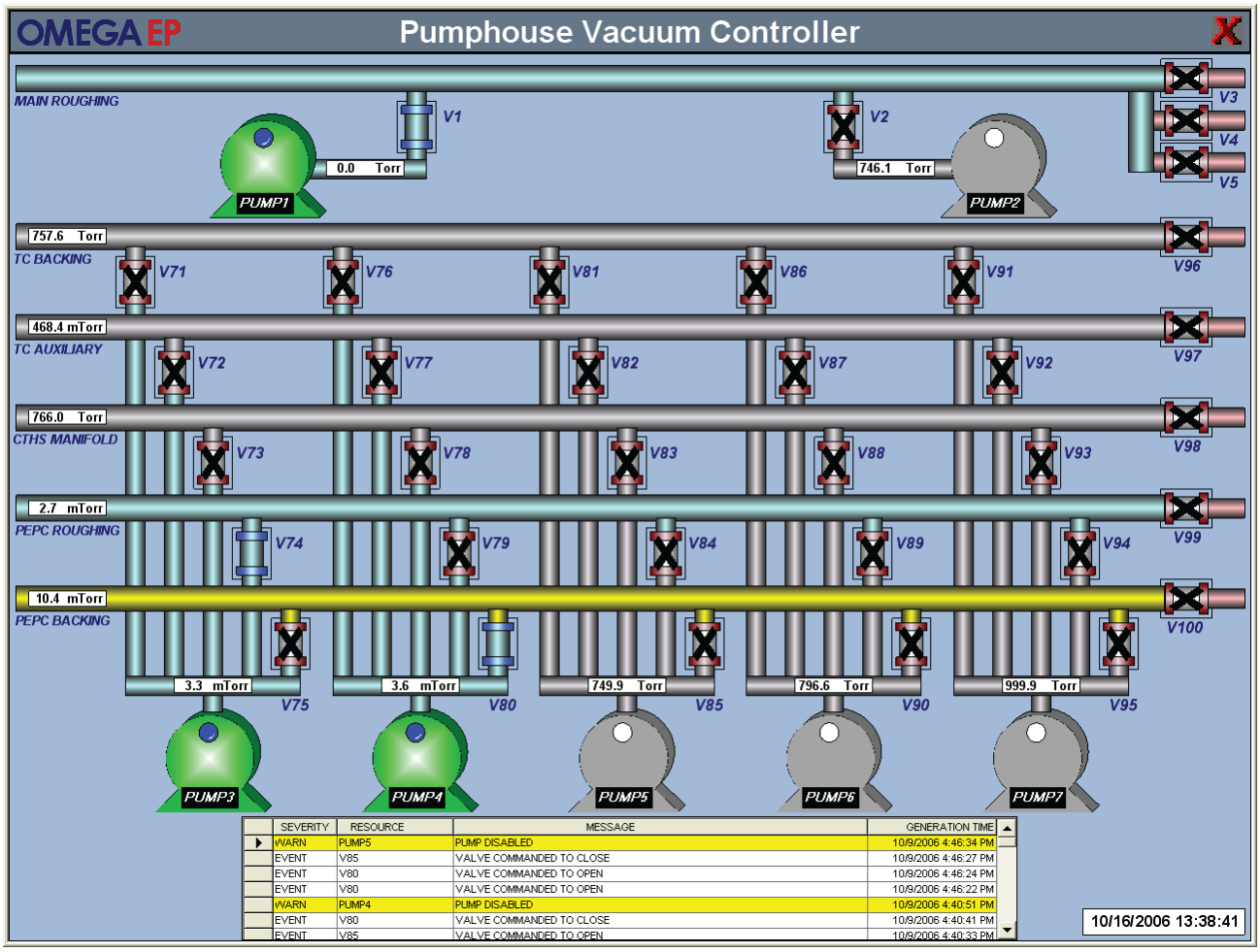

G7584J1

Figure 5.43
Pumphouse vacuum GUI showing the two main roughing pumps, the interconnect manifold, and the five auxiliary roughing pumps. The GUI is color coded to indicate the status of each pump or manifold.

The beamline spatial filter GUI allows the Beamlines Operator to control the vacuum conditions within TSF and CSF. Gate valves on either side of the pinhole vessel can be closed to isolate the tubes for easy access to the optical tables without venting the tubes themselves. The GUI, shown in Fig. 5.44, provides easy access to the gate and purge valves and permits the cryopumps to be regenerated on demand.

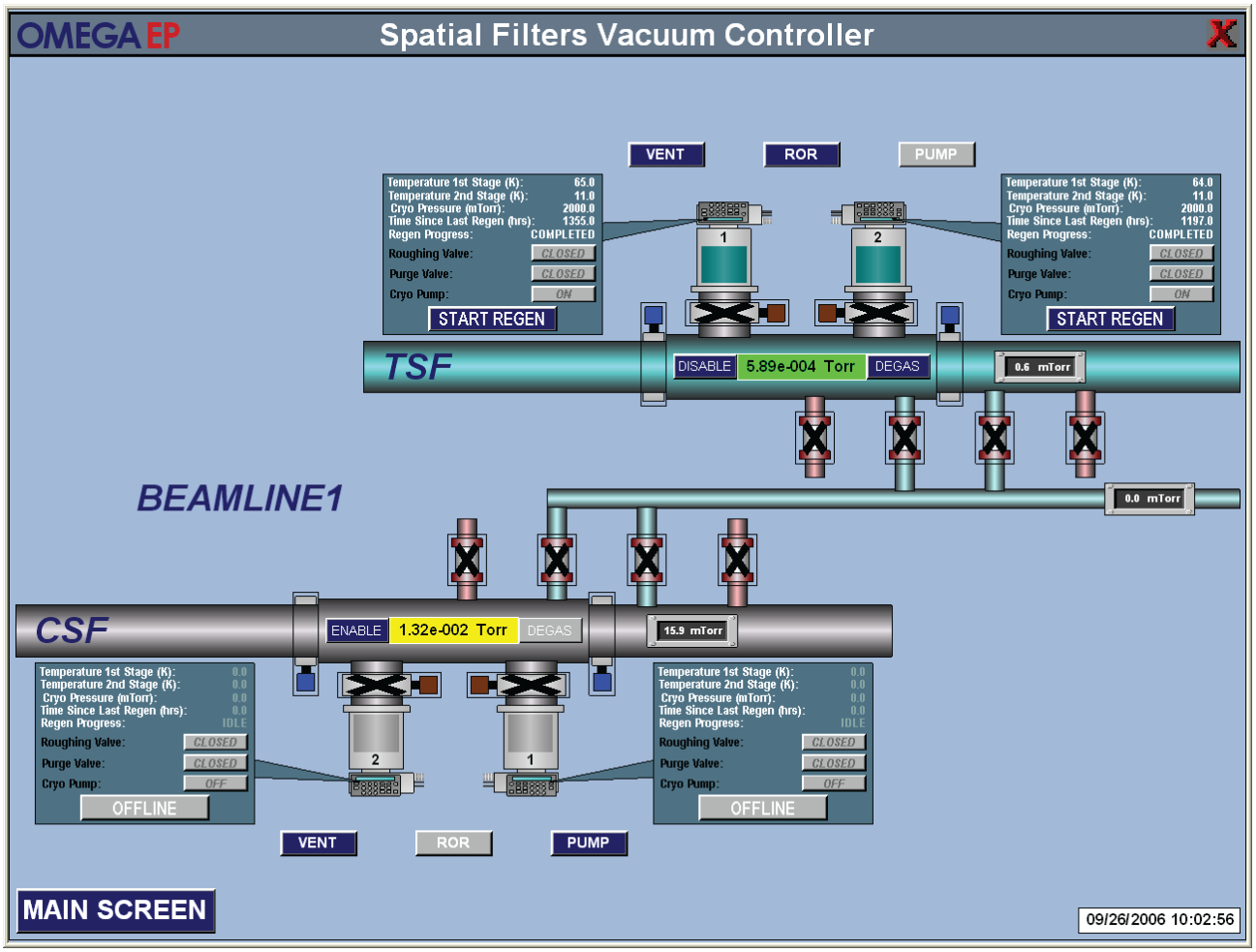

G7585J1

Figure 5.44
The spatial-filter vacuum GUI provides the operator status information and control.

The beamline enclosure GUI (Fig. 5.45) is accessed through the spatial filters GUI main screen and displays the status of enclosure doors, humidity, and high-flow nitrogen. Feeds to the high-flow nitrogen are shut off manually when access is required. More detailed information on the beamline enclosures can be found in OMEGA EP Beamline Enclosures FDR, B-DQ-M-078, Distribution, Primary Circuit Interconnect Diagram, B-DQ-I-082, and Beamline Enclosure Access Procedures, S-AB-P-152.

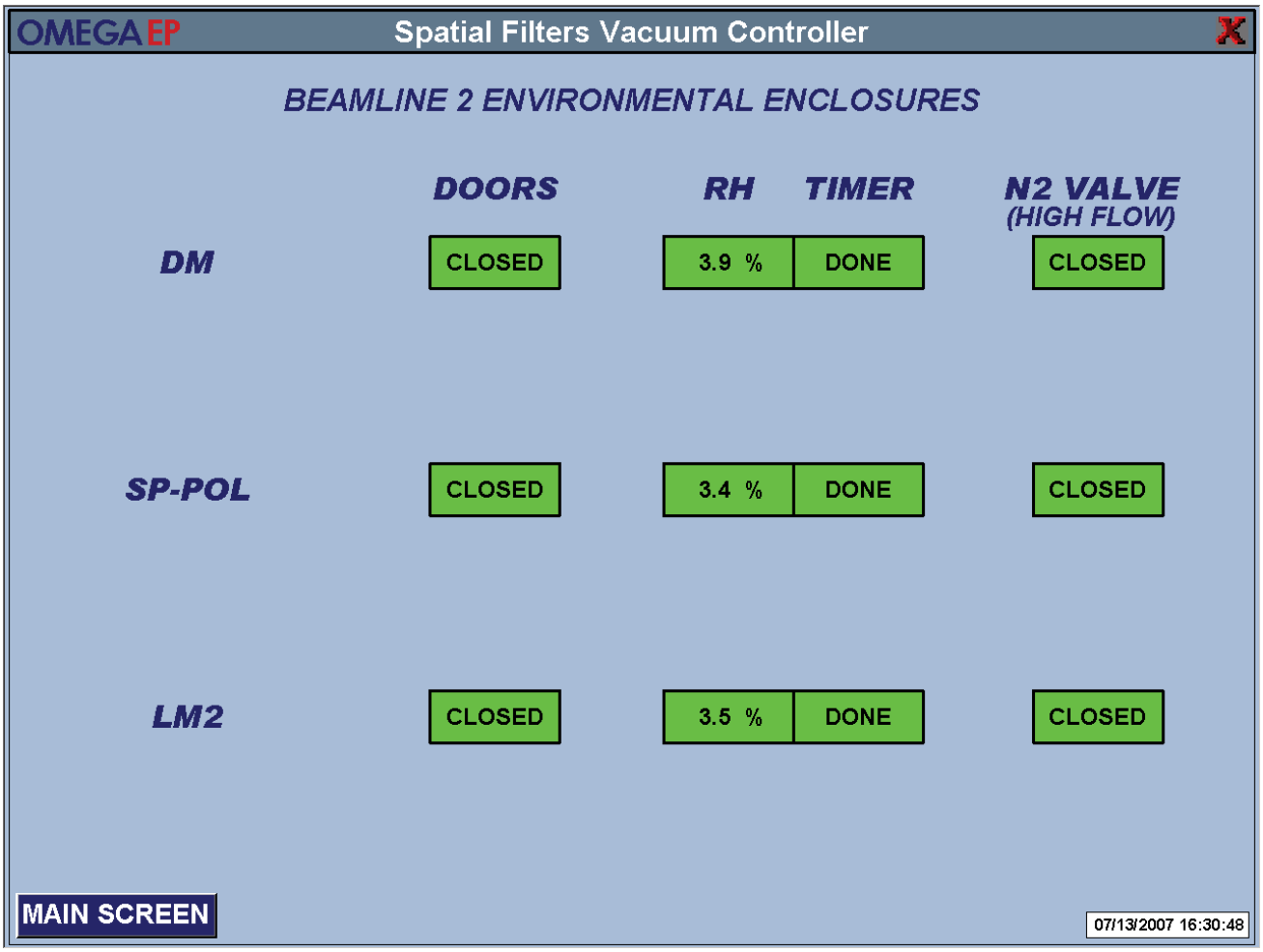

G7749J1

Figure 5.45
Spatial-filter GUI, BL2 environmental enclosures screen monitors the status of Beamline 2's enclosure doors, relative humidity, and high-flow nitrogen. The timer indicates minutes of hold time remaining until ready for shot. The GUI's for Beamlines 1 and 2 are alike, whereas the GUI's for Beamlines 3 and 4 do not contain the SP-POL row of icon's since they are not configured with SP-POL's.

The Experimental System Operator has access to and controls the vacuum systems associated with the GCC and the two beam-transport tubes to the OMEGA EP Target Chamber. Figure 5.46 illustrates the GUI and its control points and features. The gate valve to the OMEGA TC can be opened with a "token" permission from the OMEGA vacuum system controller. The target chamber vacuum controller GUI is a part of the Experimental Systems Operations.

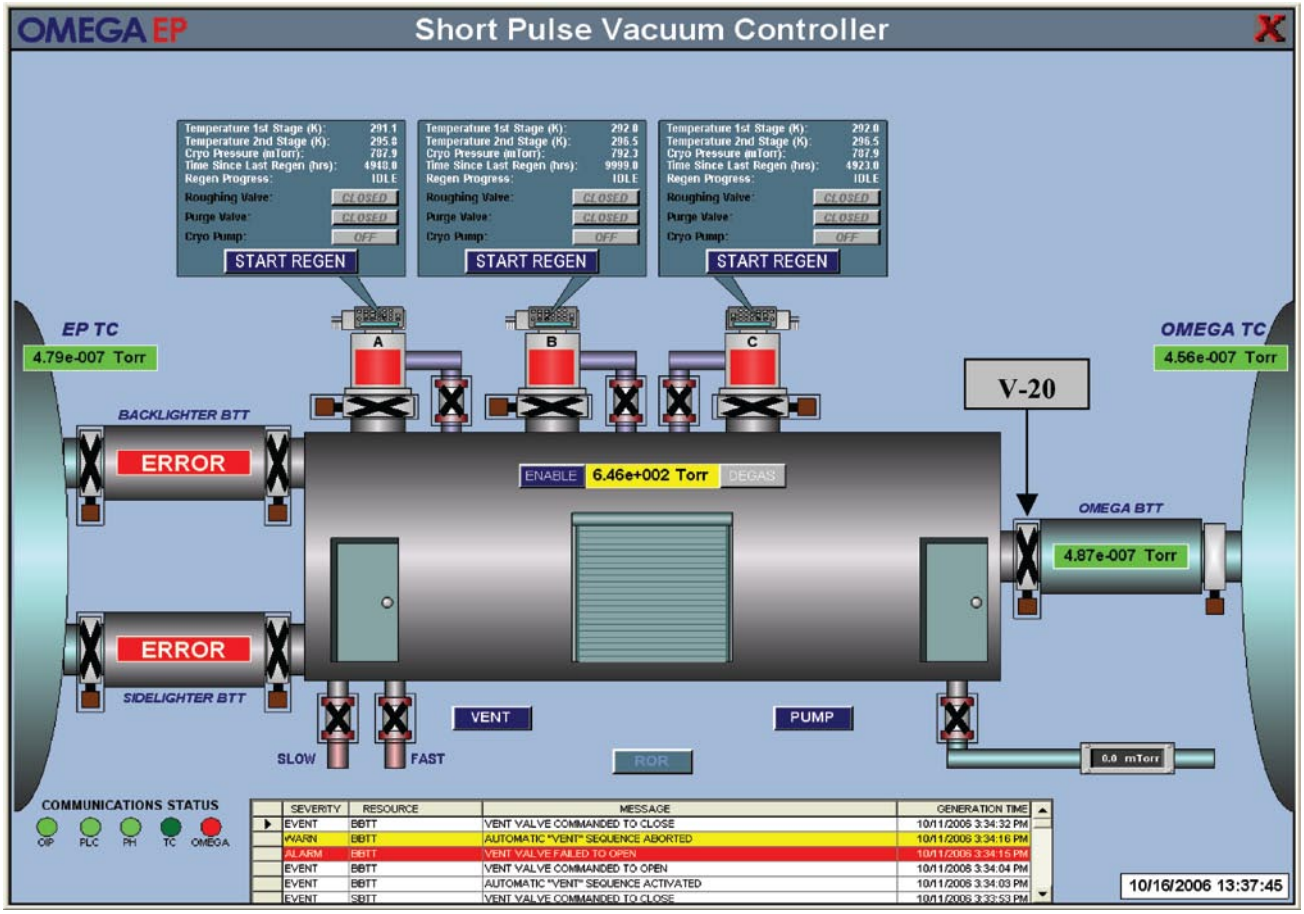

G7586J1

Figure 5.46
The short-pulse vacuum controller GUI provides the operator status information and control of the gate valves, cryo pumps, and vents. The interface between OMEGA and OMEGA EP is the isolation valve (V-20) between the beam transport tube (BTT)-to-OMEGA and the GCC.

5.4 REFERENCES

1. See "Large Optic Mounts: Technical Requirements Document," S-AC-R-008 (2 March 2006).

2. "OMEGA EP Spatial Filters: Conceptual Design Review," B-DJ-M-079 (12 July 2005); "OMEGA EP Spatial Filters Structures: Preliminary Design Review," B-DJ-M-080 (11 July 2005); "OMEGA EP Spatial Filters Structures: Final Design Review," B-DJ-M-081 (11 July 2005).

3. For a detailed drawing of the CSF pinhole assembly, see "OMEGA EP Pinhole Manipulator, CSF," B-DC-B-051 (22 May 2007).

4. R. A. Sacks, J. M. Auerbach, E. S. Bliss, M. A. Henesian, J. K. Lawson, K. R. Manes, P. A. Renard, J. T. Salmon, J. B. Trenholme, W. H. Williams, S. Winters, and R. A. Zacharias, "Application of Adaptive Optics for Controlling the NIF Laser Performance and Spot Size," in *Third International Conference on Solid State Lasers for Application to Inertial Confinement Fusion*, edited by W. H. Lowdermilk (SPIE, Bellingham, WA, 1999), Vol. 3492, p. 344.

5. M. A. Rhodes, B. Woods, J. J. DeYoreo, D. A. Roberts, and L. J. Atherton, "Performance of Large-Aperture Optical Switches for High-Energy Inertial-Confinement Fusion Lasers," Appl. Opt. **34**, 5312 (1995).

6. "High-Contrast Plasma-Electrode Pockels Cell (PEPC)," *LLE Review Quarterly Report* **107**, 129, Laboratory for Laser Energetics, University of Rochester, Rochester, NY, LLE Document No. DOE/SF/19460-696, NTIS Order No. PB2007-106962 (2006). (Copies may be obtained from the National Technical Information Service, Springfield, VA 22161.)

7. "OMEGA Hardware Timing System Software with Quad Channel Delay Module," S-AA-K-044 (14 July 2004).

8. E. B. Treacy, "Optical Pulse Compression with Diffraction Gratings," IEEE J. Quantum Electron. **QE-5**, 454 (1969).

9. "Demonstration of Real-Time, Phase-Locked Alignment of Tiled Gratings for Chirped-Pulse–Amplified Lasers," *LLE Review Quarterly Report* **100**, 242, Laboratory for Laser Energetics, University of Rochester, Rochester, NY, LLE Document No. DOE/SF/19460-578, NTIS Order No. PB2006-106672 (2004). (Copies may be obtained from the National Technical Information Service, Springfield, VA 22161.)

10. The alignment tolerances are specified in the "OMEGA EP Tiled Grating Assembly: Technical Requirements Document," B-DL-R-006 (19 October 2005).

11. The presence of deuterium in the crystal has been shown to reduce the amount of stimulated Raman scattering (SRS): J. Campbell *et al.*, "Large Aperture High-Damage Threshold Optics for Beamlet," ICF Quarterly Report **5**, (1), 68–79.

12. R. S. Craxton, "High Efficiency Frequency Tripling Schemes for High Power Nd:Glass Lasers," IEEE J. Quantum Electron. **QE-17**, 1771 (1981).

13. D. C. Brown, "Nonlinear Effects in High-Peak-Power Nd:Glass Laser Systems," in *High-Peak-Power Nd:Glass Laser Systems*, edited by D. L. MacAdam, Springer Series in Optical Sciences (Springer-Verlag, Berlin, 1981), Chap. 7, Vol. 25, p. 188.

14. "OMEGA EP UV Focus Lens," B-ED-C-002 (27 September 2005).

15. "OMEGA EP UV Optical Substrates: Technical Requirements Document," B-ED-R-005 (19 September 2005).

16. T. J. Kessler, Y. Lin, J. J. Armstrong, and B. Velazquez, "Phase Conversion of Lasers with Low-Loss Distributed Phase Plates," in *Laser Coherence Control: Technology and Applications*, edited by H. T. Powell and T. J. Kessler (SPIE, Bellingham, WA, 1993), Vol. 1870, p. 95.

17. "OMEGA EP Vacuum Window," B-ED-C-003 (28 November 2005).

18. "OMEGA EP Debris Shield," B-ED-C-004 (27 September 2005).

19. "OMEGA EP Beamline Component Installation and Alignment Plan," M-AB-Z-003 (11 January 2006).

20. "OMEGA EP Pointing Budget," S-AC-X-005 (24 April 2006); "OMEGA EP Centering Budget," S-AC-X-017 (7 October 2004).

21. "OMEGA EP Beamlines Structures Technical Requirements Document," S-AC-R-007 (1 March 2005).

22. "OMEGA EP Conceptual Design Report," Chap. 7, p. 7.7, S-AD-M-015 (June 2003).

23. "OMEGA EP Target Chamber: Technical Requirements Document," B-DM-R-001 (16 January 2004).

24. "OMEGA EP Target Area Structure Requirements: Technical Requirements Document," B-DM-R-199 (17 May 2005).

25. "OMEGA EP Grating Compressor Chamber: Technical Requirements Document," B-DL-R-001 (1 November 2003).

26. "OMEGA EP GCC Internal Structures: Technical Requirements Document," B-DL-R-025 (16 September 2005).

27. "OMEGA EP Roughing Vacuum System Requirements," D-AC-R-013 (20 April 2007).

28. "OMEGA EP Primary Circuit Interconnect Diagram," D-AC-I-009 (20 November 2006).

29. "OMEGA EP Auxiliary Circuit Interconnect Diagram," D-AC-I-010 (20 November 2006).

30. "OMEGA EP Vacuum Control System Requirements Definition," C-AG-R-001 (6 April 2006).

Appendix A OMEGA EP Beamlines Optical Component Specifications

Component	Qty	Material	Thickness (mm)	Clear aperture		Angle of incidence	Coating		Focal length (m)
				X (mm)	Y (mm)		S1	S2	
Injection subsystem									
Periscope upper fold mirror	4	BK7	25.4	138	(diam)	45°	1ω HR	N/A	N/A
LC waveplate substrate	16	fused silica	14.7	115	(diam)	0°	(a)	$R < 0.5$	N/A
Injection/IRAT beamsplitter	4	fused silica	25.4	138	(diam)	55.4°	(b)	$R_s < 0.10$ $T_s > 99.5$	N/A
Energy diagnostic pickoff	4	fused silica	25.4	138	(diam)	45°	none	none	N/A
Injection fold mirror 1	4	BK7	25.4	138	(diam)	55.4°	1ω HR	N/A	N/A
Injection fold mirror 2	4	BK7	25.4	138	(diam)	45°	1ω HR	N/A	N/A
Injection fold mirror 3	4	BK7	25.4	138	(diam)	45°	1ω HR	N/A	N/A
Injection diagnostic beamsplitter	4	fused silica	25.4	138	(diam)	45°	(c)	(d)	N/A
Injection pointing/centering mirror	8	BK7	25.4	138	(diam)	22.5°	1ω HR	N/A	N/A
Injection lower fold mirror	4	BK7	12.7	76	(diam)	45°	1ω HR	N/A	N/A
Injection upper fold mirror	4	fused silica	9.5	35	20	45°	1ω HR	N/A	N/A
Wavefront sensor pickoff	4	fused silica	25.4	138	(diam)	45°	none	none	N/A
Injection lens 1	4	fused silica	18	90	(diam)	0°	1ω AR	1ω AR	0.98
Injection lens 2	4	fused silica	15	70	(diam)	0°	1ω AR	1ω AR	1.01
Injection vacuum window	4	fused silica	12.7	102	(diam)	0°	1ω AR	1ω AR	N/A
Amplifier cavity									
Cavity deformable mirror	4	BK7	56	395	395	0°	1ω HR	none	N/A
Amplifier slab (main and booster)	72	LHG-8	41	400	752	56.4°	none	none	N/A
Cavity spatial filter lens	8	fused silica	46	406	406	0°	1ω AR	1ω AR	11.8
Short-pulse polarizer	8	fused silica	40	400	752	55.4°	1ω AR	1ω AR	N/A

Component	Qty	Material	Thickness (mm)	Clear aperture		Angle of incidence	Coating		Focal length (m)
				X (mm)	Y (mm)		S1	S2	
Amplifier cavity									
Switch polarizer	4	BK7	90	396	716	56.4°	1ω AR	1ω AR	N/A
PEPC switch window	8	fused silica	41	397	397	0°	1ω AR	1ω AR	N/A
PEPC switch crystal	4	KDP	10	397	397	0°	1ω AR	1ω AR	N/A
Cavity end mirror	4	BK7	80	392	392	0°	1ω HR	N/A	N/A
Cavity fold mirror	4	BK7	80	396	719	33.6°	1ω HR	N/A	N/A
Transport spatial filter lens	8	fused silica	56	406	410	0°	1ω AR	1ω AR	19.0
IR Diagnostic beamsplitter	4	fused silica	10	406	410	0°	(e)	1ω AR	N/A
Short-pulse beamlines									
Compressor vacuum window	2	fused silica	52	397	397	0°	1ω AR	1ω AR	N/A
Compressor input fold mirror	2	BK7	80	472	580	45°	1ω HR	N/A	N/A
Diffraction grating tile	24	fused silica	100	400	464	72.5°/61.5°	(f)	N/A	N/A
Compressor deformable mirror	2	BK7	56	395	395	10°	1ω HR	N/A	N/A
Lower comp. diagnostic mirror	1	fused silica	40	400	580	45°	1ω HR	1ω AR	N/A
Upper comp. diagnostic mirror	1	fused silica	40	400	752	55.4°	1ω HR	1ω AR	N/A
GCC Periscope Mirror 1	1	BK7	80	472	580	45°	1ω HR	N/A	N/A
GCC Periscope Mirror 2	1	BK7	80	410	660	45°	1ω HR	N/A	N/A
Beam combiner	1	fused silica	40	396	716	55.4°	TBD	1ω AR	N/A
Combiner output fold mirror	1	BK7	80	472	580	45°	1ω HR	N/A	N/A
Compressor output fold mirror	2	BK7	80	480	525	35°	1ω HR	N/A	N/A
Target chamber selection mirror	1	BK7	80	410	660	44°	1ω HR	N/A	N/A
Short-pulse transport mirror 1	3	BK7	100	495	760	53°	1ω HR	N/A	N/A

Component	Qty	Material	Thickness (mm)	Clear aperture		Angle of incidence	Coating		Focal length (m)
				X (mm)	Y (mm)		S1	S2	
Short-pulse beamlines									
Short-pulse transport mirror 2	3	BK7	80	472	645	48°	1ω HR	N/A	N/A
Off-axis parabola	3	fused silica	100	400	400	0°	1ω HR	N/A	1.04
Long-pulse beamlines									
IR transport mirror	12	BK7	80	410	660	45°	1ω HR	N/A	N/A
FCC crystal 2ω	4	KDP	11	400	400	0°	1ω AR	1ω/2ω AR	N/A
FCC crystal 3ω	4	KD*P	9	400	400	0°	1ω/2ω AR	3ω HR	N/A
Diagnostic pickoff	4	fused silica	10	410	406	10°	none	3ω HR	N/A
PMA mirror	5	BK7	80	495	655	45°	3ω HR	N/A	N/A
UV transport mirror	8	BK7	80	495	655	18°/28°	3ω HR	N/A	N/A
Distributed phase plate	4	fused silica	10	400	400	0°	3ω AR	3ω AR	N/A
Focus lens	4	fused silica	46	400	400	0°	3ω AR	3ω AR	3.4
Vacuum window	4	fused silica	24	405	420	0°	3ω AR	3ω AR	N/A

[a] Tantala spacer

[b] R_s = 99±0.10, T_s = 75±0.10, R_p = <2, T_p = 98. (R = Reflectance, s = s-polarized, T = Transmittance, p = p-polarized)

[c] R_p = 99±0.10, T_p = 0.75±0.10

[d] R_p < 0.10, T_p > 99.5

[e] R_s = 0.001, T_p > 0.995

[f] OMEGA EP Technical Requirements Document Compressor Diffraction Grating, B-DL-R-003

Appendix B

Glossary of Acronyms

ac	Alternating current
AR	Antireflection
ASP	Alignment sensor package
BA	Booster amplifier
BC	Beam combiner
BL	Beamline, e.g., BL1 = beamline 1, BL2 = beamline 2, etc.
BTT	Beam transport tube
BWA	Blast window assembly
CAD	Computer aided design
CAM	Compressor alignment mirror
CCD	Charge-coupled device
CEM	Cavity end mirror
CMM	Coordinate measurement machine
CSF	Cavity spatial filter
cw	Continuous wave (laser source)
DACM	Dual-axis control module
DBS	Diagnostic beamsplitter
dc	Direct current
DDS	Disposable debris shield
DM	Deformable mirror
DPP	Distributed phase plate
DPR	Distributed polarization rotator
DS	Debris shield
EMI	Electromagnetic interference
EOT	Energy-on-target
EP	Extended performance
f/o	Fiber optic
FCC	Frequency-conversion crystal
FF	Far field
FL	Focus lens
FOA	Focusing optics assembly
FWHM	Full width at half maximum
GCC	Grating compression chamber
G*n*	Grating number *n*, where *n* = 1, 2, 3, or 4
GPIB	General purpose interface bus (a communication protocol: IEEE 488.2)
GUI	Graphical User Interface
He	Helium
HMI	Human Machine Interface
HR	High reflection
HTS	Hardware Timing System
HTSSQ	Quad-channel Hardware Timing System server

HV	High voltage
HVAC	Heating, ventilation, and air conditioning
I/O	Input/output
IR	Infrared
IRAT	Infrared alignment table
IR-DBS	Infrared diagnostic beamsplitter
IRDP	Infrared diagnostics package
IRHR	Infrared high-reflection
KB	Kirkpatrick–Baez
KD*P	Potassium hydrogen-deuterium phosphate
KDP	Potassium dihydrogen phosphate
LENA	LON to ethernet network adapter
LLNL	Lawrence Livermore National Laboratory
LM2	Structure at the south end of the beamline containing POL1, CEM, and the fold mirror
LON	Local operating network
LOTF	Large Optical Test Facility
LP	Long pulse
LS*n*	Laser source from Laser Sources, where *n* = beamline 1, 2, 3, or 4
MBGB	Main building ground bar
MCS	Mirror Control System
MLD	Multilayer dielectric
MOSFET	Metal-oxide semiconductor field-effect transistor
NF	Near field
NIF	National Ignition Facility
nm	Nanometer
O_2	Oxygen
OAP	Off-axis parabola
OAPI	OAP Inserter
OAPI/M	Off-axis parabola inserter/manipulator
OFHC	Oxygen-free, gold-plated, high conductivity copper conductor
OIP	OMEGA intercommunication protocol
OPCPA	Optical parametric chirped-pulse amplification
PAD	Parabola alignment diagnostic
PCS	PEPC Control System
PEPC	Plasma-electrode Pockels cell
PFL	Pulse-forming line
PID	Prompt-induced deformation
PLC	Programmable logic controller
PMA	Periscope mirror assembly
POL1	Cavity polarizer; positioned first
POL2	Short-pulse polarizer; positioned second
PPG	Plasma-pulse generator
PUD	Power utility driver
QCDM	Quad-channel delay module
R	Reflectance

R_p	Reflectance of *p*-polarized light
R_s	Reflectance of *s*-polarized light
RH	Relative humidity
rms	Root mean square
RSS	Root sum square
SCADA	Supervisory Control and Data Acquisition
SCFM	Standard cubic feet per minute
SCR	Silicon controlled rectifier (General Electric's trade name for a type of thyristor)
SDIP	Structure-to-device interface package
SH	Shack–Hartmann
SHS	Shack–Hartmann wavefront sensor
SH-SS	Shack–Hartmann Sensor Service
SL	Sidelighter
SLTA	Serial LON (local operating network) talk adapter
SP	Short pulse
SPDP	Short-pulse diagnostic package
SPG	Switch-pulse generator
SP-POL	Short-pulse polarizer
SPHR	Short-pulse, high-reflection
SRF	Shot Request Form
SS-SPG	Solid-state switch-pulse generator
SSA	Single-segment amplifier
SY	Switchyard
T	Transmittance
T_p	Transmittance of *p*-polarized light
T_s	Transmittance of *s*-polarized light
TAS	Target area structure
TC	Target chamber
TCC	Target chamber center
TGA	Tiled-grating assembly
TGATS	Tiled-Grating-Assembly Test System
TIM	Ten-inch manipulator
TPS	Target Positioning System
TSF	Transport spatial filter
TVS	Target Viewing System
UV	Ultraviolet
UVAT	Ultraviolet alignment table –or– ultraviolet alignment table
UV-DBS	Ultraviolet diagnostic beamsplitter
UVDP	Ultraviolet diagnostic package
UVHR	Ultraviolet high reflection
VME	Versa Module Eurocard (a 32-bit bus that was developed by Motorola, Signetics, Mostek, and Thompson CSF)
VW	Vacuum window
WCS	Wavefront Control System
WFS	Wavefront sensor